Molecules coadsorbed on metal surfaces: Investigations using X-ray photoelectron spectroscopy

A Thesis submitted in partial fulfillment of the requirement of the degree of Master of Science as a part of the Integrated Ph.D program

by
S. Vijayalakshmi

to
Manipal Academy of Higher Education

Through

Jawaharlal Nehru Centre for Advanced Scientific Research
Bangalore
April 2002

Statement

Certified that the work described here has been done under my supervision at Jawaharlal Nehru Centre for Advanced Scientific Research, Jakkur.

Dr. G. U. Kulkarni

Dedicated

to

my parents

Acknowledgments

It gives me great pleasure to express my gratitude and respect to Prof. G.U. Kulkarni for his day to day guidance in the field of Surface Science. He has always been encouraging and I would like to thank for his advice and keen interest in my academic welfare. I would like to thank Prof. C.N.R. Rao FRS for giving me opportunity to work in close association, introducing me to this field and also for his encouragement.

I am grateful to my senior Mr. C.P. Vinod for teaching me the surface science techniques and helping me in handling the instrument. I am thankful for his unconditional help.

Special mention to Messrs. Srinath and Srinivas for attending the problems in the instrument promptly and without reluctance.

I would like to acknowledge the tutors of the courses both in JNC and IISc whose teachings were very fruitful.

I like to thank Complab for providing computational facilities.

Thanks to all of my friends in IISc and JNC and my seniors for making my stay comfortable. I would like thank Anupama and Sivashankar especially for helping me in the coursework and their constant encouragement. It was great pleasure having John and Neena as my labmates.

My heartfelt thanks to Pushpa who has been a good friend of mine and I am grateful for her tremendous help and moral support. I am grateful to my brother-in-law, my elder sister and my younger sisters for their love and affection. The thesis would be incomplete without acknowledging my beloved parents for allowing me to continue my studies as the way I wished and for providing me all the comforts that I needed. I dedicate this thesis to them.

CONTENTS

Statement ii
Acknowledgements iv
Contents vi
Summary vii
List of abbreviations ix

Chapter 1

Surface chemistry

1.0 Introduction 1
1.1 Single crystal metal surfaces 1
1.2 Adsorption of gas molecules 5
1.3 Interaction of molecules with metal surfaces 10
1.4 Coadsorption of gases 15
1.5 Experimental methods 18
1.6 Scope of the present investigation 29
1.7 References 31

Chapter 2

A hydrogen bonded methanol-water complex on Zn(0001) surface

2.1 Introduction 34
2.2 Experimental 35
2.3 Results and Discussion 36
2.4 Conclusions 46
2.5 References 47

Chapter 3

Interaction between carbon disulphide and oxygen on a Ni(110) surface

3.1 Introduction 48
3.2 Experimental 49
3.3 Results and Discussion 49
3.4 Conclusions 60
3.5 References 61

Summary

Two aspects related to surface chemistry of molecules have been dealt with in the thesis. The first one pertains to stabilization of molecular methanol on a Zn(0001) surface by coadsorbing water. X-ray photoelectron spectroscopy measurements were carried out after exposing the Zn surface at 80K to the binary vapor from water-methanol liquid mixtures of varying compositions and subsequently warming the surface upto the room temperature. When the surface was exposed to the vapor from a mixture with water molefraction, x_w, of 0.5, the proton abstraction and the C-O bond cleavage in methanol leading to methoxy (CH_3O) and the hydrocarbon (CH_x) species respectively, occured at a much higher temperature of 180K, compared to 120K in the case of pure methanol adsorption. For water rich mixtures (x_w = 0.7 and 0.9) molecular methanol was stabilized on the surface upto 200K, beyond which water itself desorbed. For x_w = 0.7, virtually no dissociation was observed upto 200K. The increased stability of molecular methanol on Zn(0001) surface is attributed to the surface mediated hydrogen bonds that stabilize a water-methanol complex.

The second aspect addresses the nature of adsorption of CS_2 on Ni(110) surface in the pure form as well as in mixtures containing oxygen. Pure CS_2 adsorbs dissociatively giving rise to graphitic carbon (C1s, 285eV), chemisorbed sulphur (S2p, 164eV) and perhaps a small proportion of CS(a) (C1s, 286eV). A CS_2-O_2 mixture dilute in oxygen (220:1) gave rise to a new species COS(a) (O1s, 534eV) due to the reaction between the transients, O^{1-}(s) and CS(s). The COS(a) species was also formed in the case of a 15:1 CS_2-O_2 mixture, the other prominent species on the surface being O^{1-}(a) (531eV). When a mixture with comparable compositions of CS_2 and O_2 (2:1) was dosed, mainly O^{2-}(oxidic) species (O1s, 530eV) was formed with no evidence of sulphur on the surface.

When O_2 and CS_2 were dosed in a sequential manner, there was some formation of COS(a). On the other hand, when O_2 was dosed on a surface predosed with CS_2, oxygen adsorption was inhibited.

Papers based on this work have been submitted to *ChemPhysChem* and *Catal. Lett*.

List of Abbreviations

CCP Cubic Close Packing

EELS Electron Energy Loss Spectroscopy

FIM Field Ion Microscopy

HCP Hexagonal Close Packing

LEED Low Energy Electron Diffraction

PES Photo Electron Spectroscopy

STM Scanning Tunneling Microscopy

TPD Temperature Programmed Desorption spectra

UHV Ultra High Vacuum

UPS Ultraviolet Photoelectron Spectroscopy

XPS X-ray Photoelectron Spectroscopy

1. Introduction

Condensed phases-solids and liquids must have surfaces or interfaces. These surfaces exhibit some remarkable physical and chemical properties, which may significantly differ from those of the bulk [1]. The importance of surface science and in particular surface chemistry has been recognized for nearly two centuries [2] mostly in connection with heterogeneous catalysis. The earliest attempt was perhaps by Dobereiner in early 18^{th} century, associated with the discovery of Pt surface catalyzed reaction of H_2 and O_2. Over the decades surface science has evolved into an important branch of science due to seminal contributions from Kirchhoff, Davy, Henry, Philips, Faraday, Berzelius, Deacon, Messel, Mond, Ostwald, Sabatier, Haber, Langmuir and many others. Since 1950's the availability of ultrahigh vacuum systems and solid state electronic circuitry resulted in the fast growth of the discipline into the present modern surface science. New instrumentation methods and techniques that have been developed in the last few decades indeed permit the study of surface properties on an atomic scale.

1.1 Single crystal metal surfaces

The industrial processes involve the use of catalyst in the form of highly dispersed powders. However, the basic understanding of simple catalytic reactions at a microscopic level is possible only with well-defined single crystal surfaces. This involves preparing a flat, usually low Miller index, face of a single crystal of the material of interest and studying the adsorption or co-adsorption of molecules on them in an otherwise ultrahigh vacuum environment (3).

In simple terms, one can visualize a well-oriented surface formed as a result of a cleavage along a crystallographic plane of the bulk crystal. The surface atoms will then exhibit

more or less unsaturated valencies with a strong tendency for lowering the energy, e.g. by chemical bond formation with molecules arriving from the gas phase. Thus, a substrate surface can be defined as the plane below which a 3-dimensional periodicity and all the properties of the bulk apply and surface as the region above this plane where the geometric, chemical, electronic and vibrational properties are different from those of the bulk. Interest in surface science is, in general, motivated by this diversity in properties exhibited by various surfaces compared to the bulk [3].

Most of the technologically important metals possess face centered cubic (fcc) structure. For example, the catalytically important precious metals (Pt, Rh, Pd) all exhibit fcc structure. Reactive metals such as Cu and Ni also exist in fcc structure. Their low index planes of most frequently studied are (100), (110) and (111). The fcc(100) is obtained by cutting the fcc metal parallel to the front surface of the fcc cubic unit cell. This exposes a surface with an atomic arrangement of 4-fold symmetry. The fcc(110) surface is obtained by cutting fcc unit cell in a manner that intersects the x and y-axes but not the z axis- this exposes a surface with an atomic arrangement of 2-fold symmetry. The (111) surface of an fcc metal is obtained by cutting the fcc metal in such way that the surface plane intersects the x, y and z axes at the same value-this exposes a surface with an atomic arrangement of 3-fold symmetry [4]. The atomic arrangement in the three fcc surfaces is shown in Fig.1.1.1.

The important class of hcp structure includes metals such as Ti, Co, Zn and Ru. The (0001) surface is the most straightforward of the hcp surfaces since it is obtained by cutting the hcp metal in a way that intersect the c-axis. This plane is coplanar with other 3 axes and is also sometimes referred to as the (001) surface. Fig.1.1.2 shows the hcp(0001) surface.

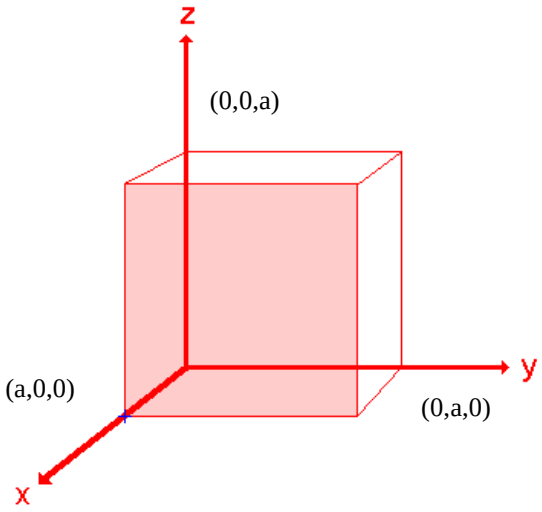

fcc(100)

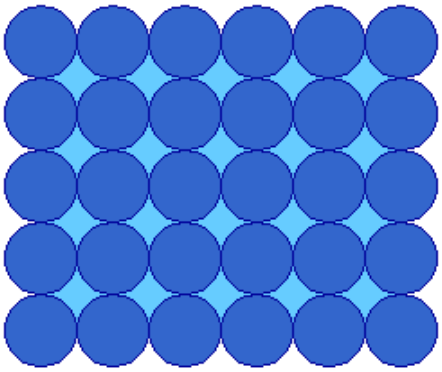

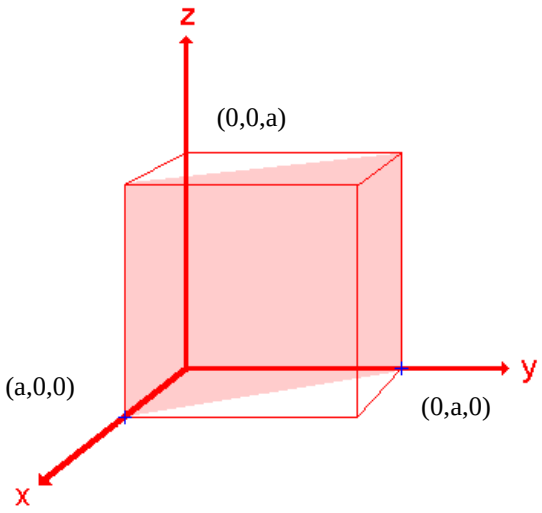

fcc(110)

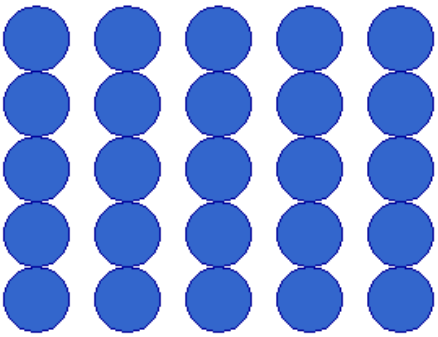

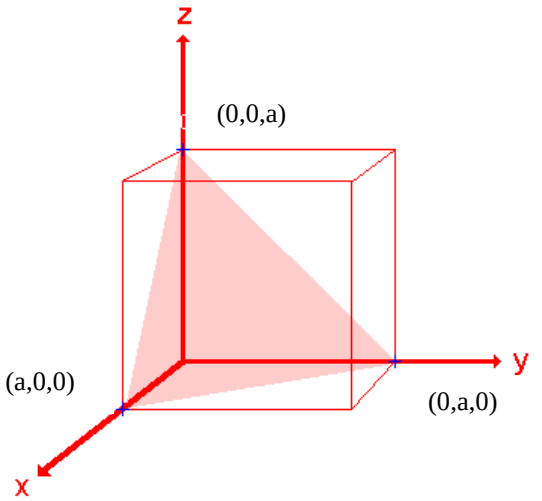

fcc(111)

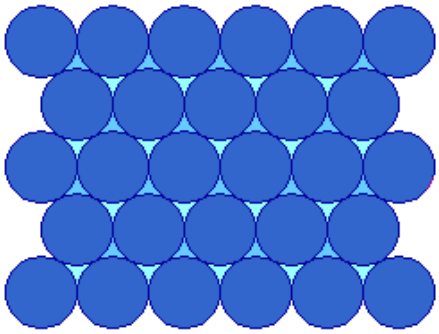

Fig. 1.1.1 Arrangement of atoms in (100), (110) and (111) surfaces of a fcc metal. The [100], [110] and [111] crystallographic directions are perpendicular to the corresponding plane.

hcp(0001)

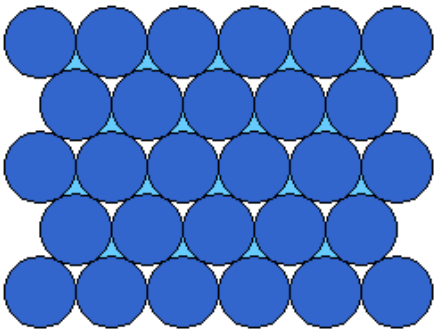

Fig. 1.1.2. Arrangement of atoms in an hcp(0001) surface. The [0001] crystallographic direction is perpendicular to the plane

An ideal single crystal surface is infinitely smooth and does not contain any defect. But in reality, we cannot have a single crystal plane without defects (Fig.1.1.3). The steps and kinks that occur on the surface often limit the width of the terrace from few tenths to few hundred nanometers [5]. An example of a Cu(110) surface is shown in Fig. 1.1.3.

The reactivity of a given metal is different on its different surfaces. The reactivity depends inversely on the co-ordination number of the surface atom. For fcc surfaces, the reactivity follows the trend 110 > 100 > 111, the co-ordination numbers being 7, 8 and 9 respectively. Compared to a plain smooth surface, a rough surface has lot of defect sites and hence shows much higher reactivity. On a rough surface, the kink site is the most reactive, the step and the terrace sites exhibit much less reactivity which again shows the primary role of the surface coordination number in the reactivity of a surface.

a) b)

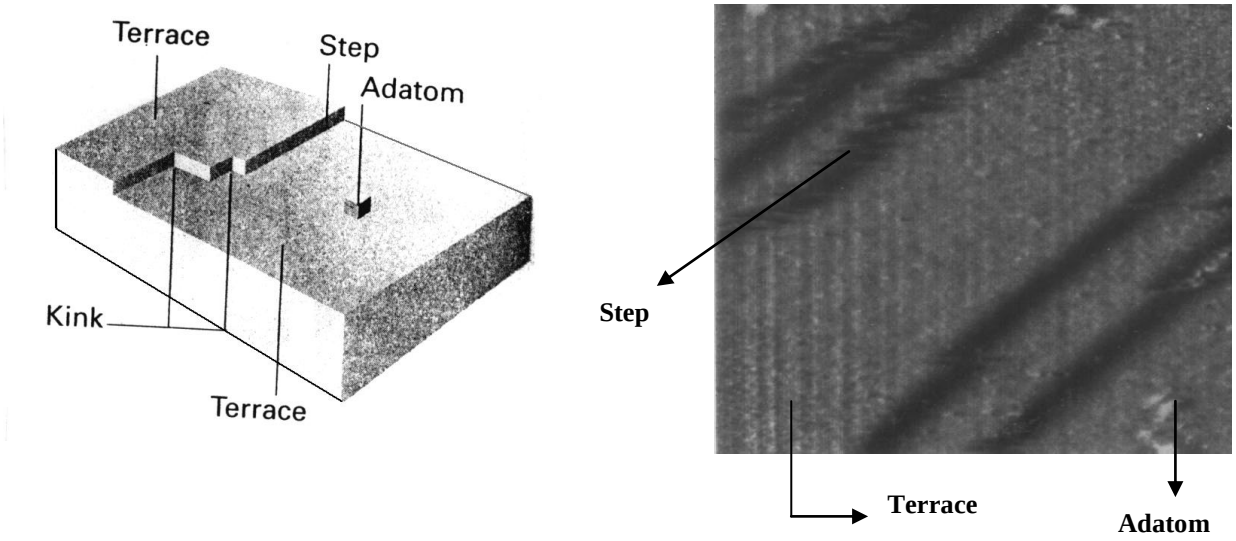

Fig.1.1.3 a) Defect sites on a single crystal surface
b) Scanning Tunneling Micrograph of a Cu(110) single crystal (from A.F. Carley, P.R. Davies, R.V. Jones, G.U. Kulkarni and M.W. Roberts, Chem. Comm. 687 (1999)).

1.2 Adsorption of gas molecules

Adsorption is a process by which the foreign atoms and molecules attach themselves to the atoms at the surface of the substrate. These foreign atoms and molecules are called adsorbates and the surface is known as adsorbent. When a metal surface is exposed to a gas containing some molecules, the nature of the surface species formed depends on how a molecule interacts with the given surface. The different processes taking place on the surface is schematically illustrated in Fig.1.2.1. It can range from a simple molecular adsorption to a complex surface reaction.

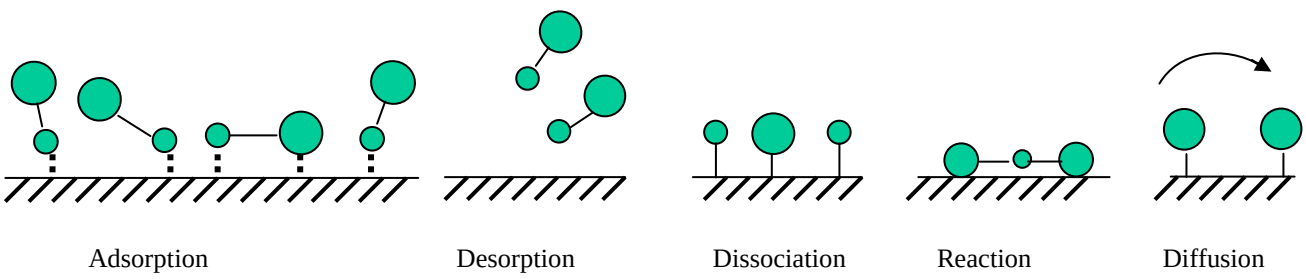

Fig.1.2.1. Schematic diagram showing the types of processes on a surface

The initial step in all surface reactions is the adsorption in which the reactants collide with the surface, stick and form an adsorbed layer. For a molecule to adsorb on a surface, some conditions have to be fulfilled. Firstly, there must exist an adsorption state with sufficiently strong bonding to the surface, strong compared to the thermal energy of the adsorbate, which is given by the surface temperature. Secondly, if an activation barrier for adsorption exists the initial energy of the colliding molecule has to be sufficiently high in order to surmount the barrier. Finally, the molecule has to loose its excessive translational energy during the collision in order not be reflected back to the gas phase. The probability that a molecule becomes adsorbed upon collision with a surface, thus, depends on details of the molecule-surface interaction - adsorption states, activation barriers and the energy-transfer processes. Accordingly, there are two principal modes of adsorption depending upon the energy of interaction between the substrate and the adsorbate, namely, physisorption and chemisorption. When the interaction of the adsorbate to the adsorbent is weak i.e. governed by attractive forces of Vander Waals, the adsorption is called physisorption.If the interaction of the substrate to the adsorbate is strong enough to result in the formation of chemical bonds or sharing of electrons then the adsorption is said to be chemisorption. The nature of this bond may lie anywhere between the extremes of virtually complete ionic or complete covalent character. In physisorption, the adsorbate-adsorbate interaction is stronger than the adsorbate-substrate interaction whereas in the case of chemisorption the latter is stronger.

On approaching the surface, each atom or molecule encounters an attractive potential that ultimately will bind it to the surface under proper circumstances (Fig.1.2.2). The potential energy diagram for the adsorption process is a representation of the variation of the energy of a system as a function of the distance (d) of an adsorbate from the surface of the substrate.

Fig.1.2.3 shows the typical potential energy curves for physisorption and chemisorption processes.

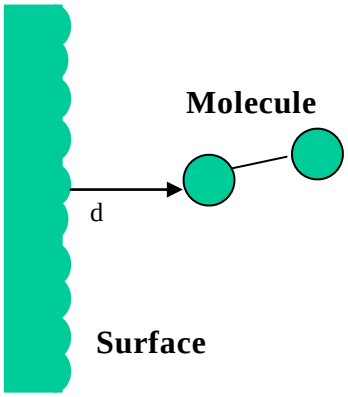

Fig.1.2.2 . Schematic diagram showing a gaseous molecule approaching the surface from the distance d (nm)

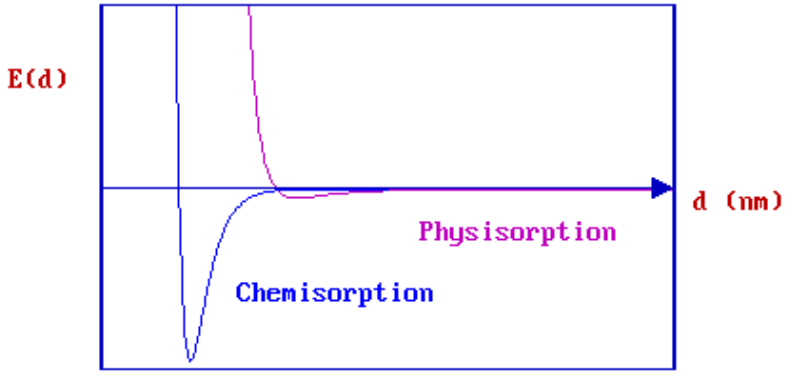

Fig.1.2.3 Potential energy diagram of a molecule for physisorbed and chemisorbed state

Physisorption d > 0.3nm ΔH_{ads} ~ -25kJ/mol

Chemisorption d < 0.3nm ΔH_{ads} ~ -150kJ/mol to -400kJ/mol

The depth of the chemisorption well is a measure of the strength of binding to the surface. The molecule approaching the surface may go through the physisorption curve and

directly get into chemisorption at the cross over point or it may desorb. Depending upon position of the crossover point with respect to the initial zero energy of the system the adsorption process may be activated or non-activated.

Mobility of the adsorbates on the substrate surfaces is the another aspect that depends on the strength of the interaction between the adsorbate and the substrate. The adsorbed species may hop from a high-energy site to a low energy site of the substrate, which is dependent on the activation energy for hopping ($E_a < kT$ or $E_a > kT$) [6]. The rate of hopping can be of the order of 10^{15} sec^{-1}. But it can vary. When there is a concentration gradient for the adsorbate on the surface, the adsorbate may diffuse towards low concentration side till the equilibrium concentration is reached. The activation energy for diffusion over a surface need not be the same as for desorption because the adsorbed species may be able to hop through valleys between potential peaks without leaving the surface completely. In general, the activation energy for migration is about 10-20% of the energy of the surface-adsorbate bond, but the actual value depends on the extent of coverage, structure of the sample, temperature and the crystal planes. For example, the activation energy for diffusion of tungsten atoms on tungston surface is shown to be in the range of 57-87 kJ/mol [5].Diffusion characteristics of an adsorbate can be examined by using STM or FIM. The STM picture in Fig.1.2.4 illustrates how a row of adsorbed oxygen diffuses to join an oxide island on a Cu(110) surface.

The adsorbent surface provides various types of sites differing in symmetry for the adsorbate molecules. These sites in turn are not similar in nature for different crystallographic planes of the same adsorbent. Fig.1.2.5 shows various sites available on different surfaces.

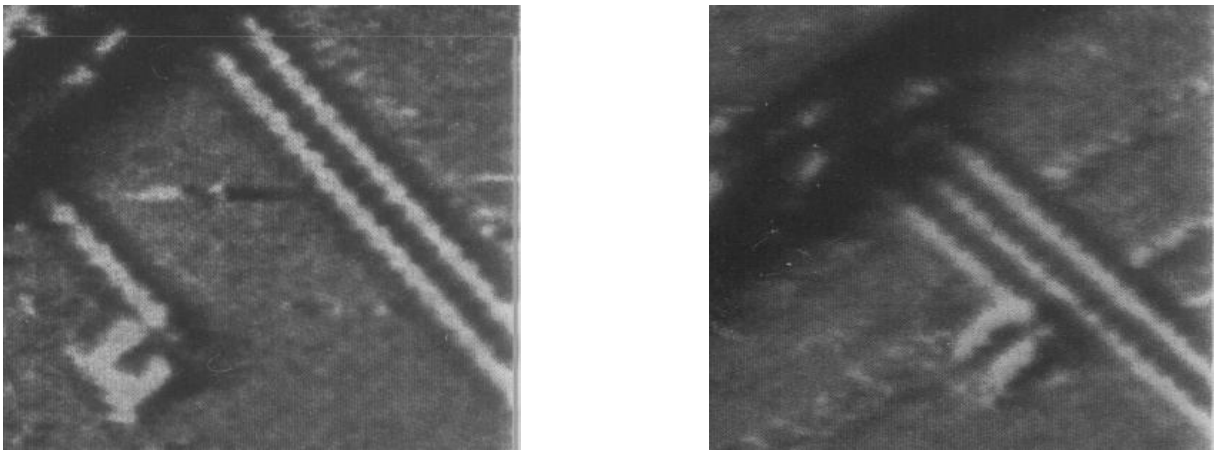

time t = 0 sec

t = 10sec

Fig.1.2.4 Images showing surface migration of the adsorbed oxygen species on the Cu(110) surface
(from A.F. Carley, P.R. Davies, R.V. Jones, G.U. Kulkarni and M.W. Roberts, Chem. Comm. 687 (1999))

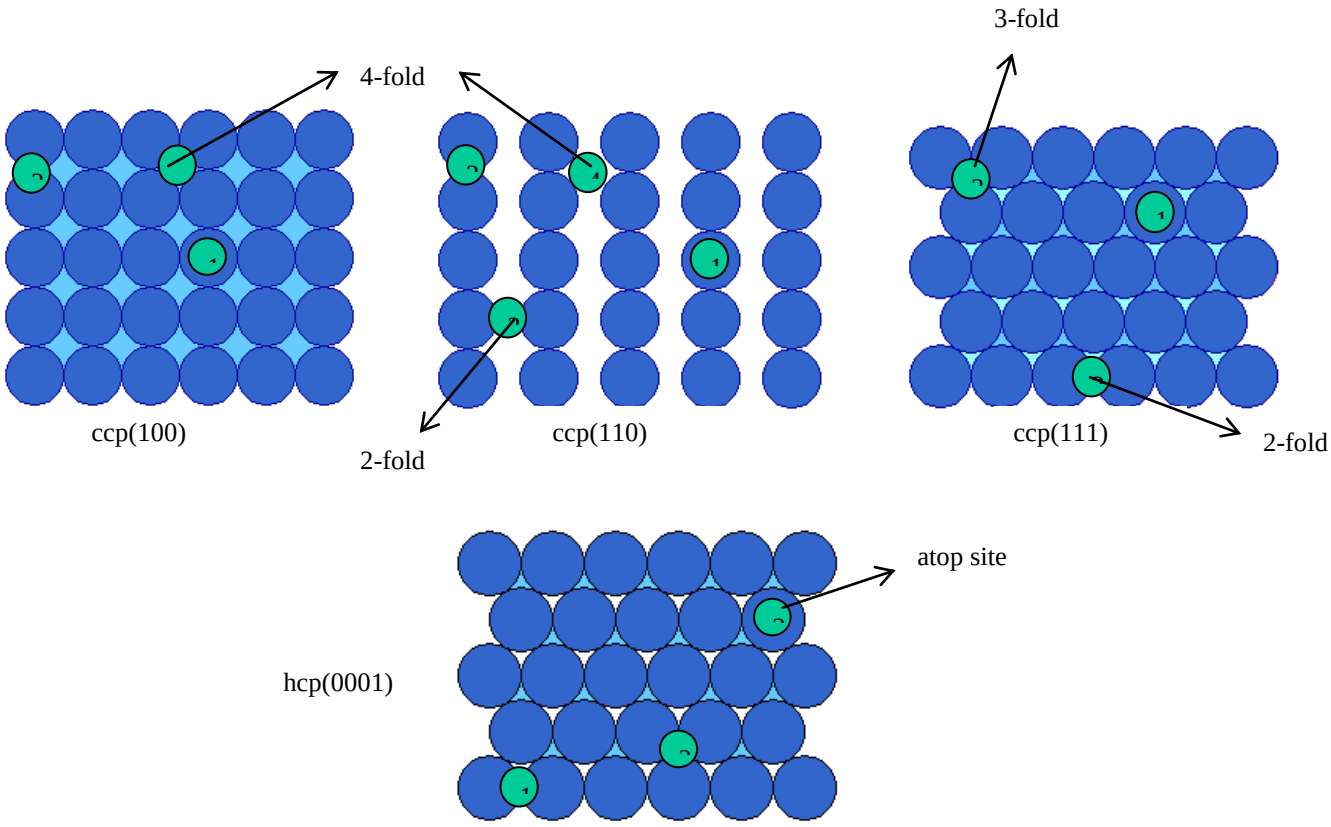

Fig.1.2.5. Various types of sites available for the adsorption of molecules on fcc and hcp surfaces

1.3 Interaction of gaseous molecules with metal surfaces

Metal surfaces exhibit diverse adsorption behavior. For example, for a given metal, the general trend is that the adsorption strength decreases along the series O_2, C_2H_2, C_2H_4, CO, H_2, CO_2 and N_2. Some of these molecules adsorb dissociatively. Elements from the d-block such as Fe, V and Cr show strong activity towards all of these gases, but Mn and Cu do not adsorb N_2 and CO_2. Metals towards the left of the periodic table such as Mg and Li can interact only with the most reactive gas like O_2. The reactivity of metals towards different molecules is summarized in the table below.

Table 1.3.1 Chemisorption abilities of metals

	O_2	C_2H_2	C_2H_4	CO	H_2	CO_2	N_2
Ti, Cr, Mo, Fe	+	+	+	+	+	+	+
Ni, Co	+	+	+	+	+	+	–
Pd, Pt	+	+	+	+	+	–	–
Mn, Cu	+	+	+	+	±	–	–
Al, Au	+	+	+	+	–	–	–
Li, Na, K	+	+	–	–	–	–	–
Mg, Ag, Zn, Pb	+	–	–	–	–	–	–

+ chemisorption ; - no chemisorption

The adsorption behavior of some simple molecules – CO, O_2, N_2 and H_2O are discussed below.

Adsorption of CO

Depending upon the metal surface, carbon monoxide may adsorb either in the molecular form or may undergo dissociation – in some cases both states coexist on particular surface planes and over specific ranges of temperature. On the reactive surfaces of metals from the

left-hand side of the periodic table (e.g. Na, Ca, Ti and rare earth metals), the adsorption is almost invariably dissociative leading to the formation of adsorbed carbon and oxygen atoms.

By contrast, on surfaces of metals from the right hand side of the d-block (for example, Cu, Ag), the interaction is predominantly molecular; the strength of interaction between the CO molecule and the metal is also much weaker, so the M-CO bond may be readily broken by raising the surface temperature without inducing any dissociation. For the majority of transition metals, however, the nature of the adsorption is very sensitive to the surface temperature and surface structure. The geometry of molecular adsorption is also varied.

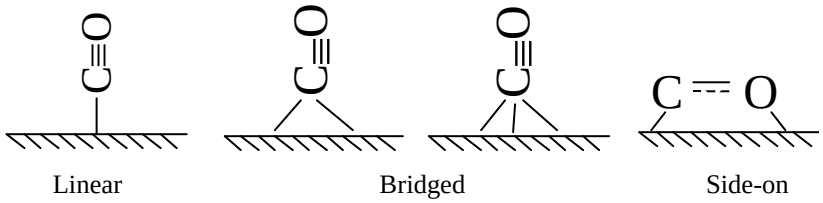

Fig.1.3.1 Schematic diagram showing different geometries of CO on transition metal surfaces

CO occupies various types of sites such as atop, 2-fold site, 3-fold hollow site, and 4-fold hollow site. But the preferred adsorption site depends upon the metal surface, crystallographic face, CO coverage and the temperature. For example, on the Ni(111) surface, CO occupies the bridge site at low coverages [7] while on Rh(111) [8] and Pt(111) [9], the top sites are preferred.

Adsorption of O_2

Oxygen usually adsorbs dissociatively on most metal surfaces. Molecular adsorption is found on some metals such as Ag and Pt. The type of adsorption is dependent on the nature of the metal surface, temperature and the extent of coverage and as many as four different species may be present on the surface [10]. Alkali metal surfaces serve as good examples. On

surfaces of Ni for example, an intermediate behavior is observed in that only O^{1-} and O^{2-} species are present [11,12,13]. At relatively high temperature and high coverage, metals generally undergo bulk oxidation [14]. The nature of the species may be sensitive to the crystallographic plane under consideration. The Ag(111) surface favors superoxo species [15] while the Ag(110) surface produces mostly the peroxo species [16,17]. On Pt polycrystalline surface, both atomic and molecular species are seen at low temperatures [18] while only molecular adsorption is observed on Pt(111) [19]. The possible adsorption geometries of the different oxygen species are shown in Fig.1.3.2.

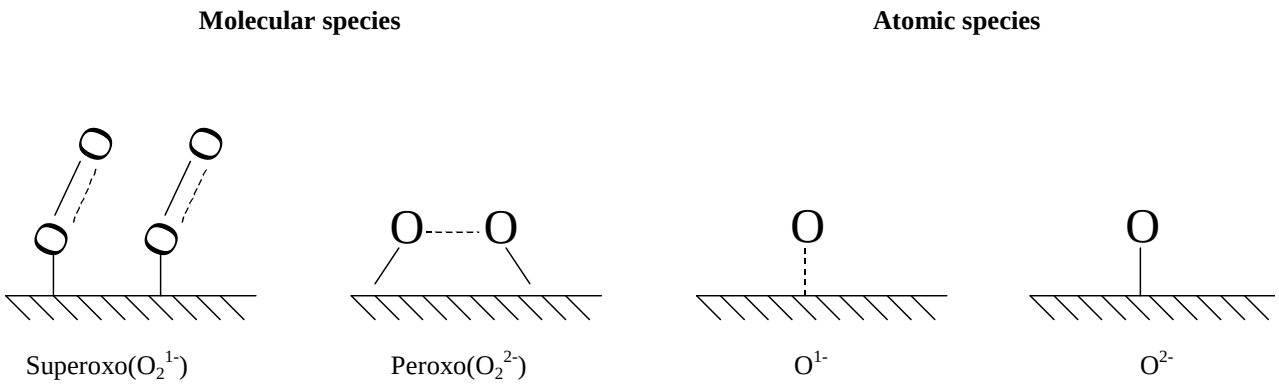

Fig.1.3.2 Schematic diagram showing the various adsorption geometries of oxygen

Molecules aligned such that the inter-nuclear axis is parallel to the surface plane may bond to a metal atom via both the s-donor interaction, in which the charge transfer is from the occupied π-bonding molecular orbital of the molecule into the vacant orbital of σ-symmetry of the metal and p-acceptor interaction, in which an occupied metal d-orbital of the correct symmetry overlaps with empty p* orbital of the molecule and in this case charge transfer is from the surface to the molecule. However in some cases, the interaction of O_2 with the surface can mitigate the high intrinsic bond energy and thereby facilitate dissociation.

Adsorption of N_2

Interaction of nitrogen with metal surfaces shows many of the same characteristics as those of oxygen [20]. However in general, N_2 is less susceptible to dissociation as a result of the lower M-N bond strength and the substantial kinetic barrier associated with breaking the N≡N triple bond. There are three basic types of strongly chemisorbed species of N_2 on the surfaces. These are: the weakly adsorbed γ state, the strongly adsorbed α state and the atomic β state. The α state turns out to be the precursor to the β state; γ be the precursor to the α state on some metal surfaces. The adsorption energies vary in the order $\beta > \alpha > \gamma$. Metals such as Fe, Ni, Cr, Ru, Mo, Ir and Rh adsorb N_2 in weak molecular states at low temperatures and dissociate into atomic species at room temperature. Most active surface of iron towards N_2 is Fe(111) [21]. The Fe(100) surface forms surface nitrides similar to bulk Fe_4N [22]. Polycrystalline Re surface is more effective than Fe(111) - it dissociates N_2 even at 80K [23-26]. On the other hand, Re(0001) is inactive [27]. The W(100) also dissociates N_2 at 90K [28]. At low temperatures, N_2 exists in both atomic and molecular states on Pt surfaces [29]. Other transition metal surfaces as Ti, Zr, Nb, Ta, V and Hf adsorb N_2 dissociatively [30,31], while Pd shows no reactivity at room temperature [32].

The Fig.1.3.3 shows the two different geometries of adsorption of N_2. The γ state is the end-on orientation while the α state is side-on orientation.

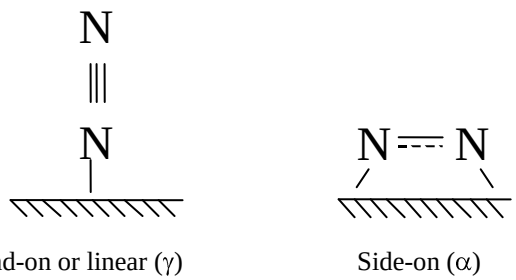

Fig.1.3.3 Schematic diagram showing various geometries of adsorption of N_2 on transition metal surfaces

Nitrogen is *iso*-electronic with CO. In contrast to CO, N_2 prefers to adsorb on transition metal surfaces only in end-one orientation. Interaction of N_2 with metal surfaces has been a topic of considerable interest for several years due to its intimate connection with ammonia synthesis.

Adsorption of H_2O

Water molecule binds with the metal surface through oxygen lone pairs. Adsorption of H_2O has been studied on many metal surfaces [33]. At low temperatures, H_2O adsorbs molecularly and forms multilayers. The first layer is the chemisorbed water on the metal. The second layer is physisorbed water and is stabilized by H-bonding with the first layer.

Water adsorbs molecularly on a Ru(0001) surface at low temperature [34]. The Pt(111), Pt(100) and Pd(100) surfaces also adsorb water molecularly [35,36]. Interestingly in the H_2O/Pt(111) system, the first layer molecules are bounded to the Pt through oxygen and also there is an evidence for the hydrogen bonding O-H---Pt since Pt shows strong affinity for hydrogen[37].

The adsorption is molecular on the Zn(0001) surface at low temperature with a desorption temperature of 200K. On Ni(110) [38,39] and Cu(110) [40] it forms dimers at low temperatures which dissociate on warming the surface to 130K giving rise to a mixture of oxide and hydroxide. Rare earth metal surfaces [41] as well as those of Mg, Al, Cr, Mn and Fe [42] are known to form a mixture of oxide and hydroxide on exposure to water. The hydroxide is abundant if the reaction takes place at low temperatures.

1.4 Coadsorption of gases

When a metal surface is exposed to a mixture of gases, the adsorption behavior may be different compared to adsorption of individual gases. In coadsorption, the intermolecular interactions involving London dispersion forces, dipole-dipole forces of interaction H-bonding as well as electronic interactions come into play often resulting in the formation of a new molecule or a surface complex. A few examples are described below.

Coadsorption of NH_3 and O_2 on Zn(0001) surface

NH_3 is unreactive on clean and oxidized Zn(0001) surfaces. But when it is coadsorbed with O_2 on Zn(0001) surface, the nature of adsorption of both the species changes [43]. NH_3 reacts with O_2 to form a complex, which then decomposes to NH_2 and OH^- species. XPS and EELS studies confirm the formation of NH_2 and OH^- species.

Reaction pathway for pure O_2 and NH_3+O_2 adsorption

$$O_2(g) \longrightarrow O_2^{\delta-}(s) \longrightarrow 2O^{2-}(a)$$

$$O_2 \longrightarrow O_2^{\delta-}(s) \xrightarrow{NH_3(g)} (NH_3\text{----}\ O_2^{\delta-})(s) \longrightarrow OH(a) + NH_2(a) + O^{2-}(a)$$

The participation of an NH_3-O_2 complex as a transition state species makes the O_2 bond cleavage faster than for pure O_2. The evidence for precursor-mediated kinetics and increased efficiency for dioxygen bond cleavage in the presence of ammonia is provided by X-ray Photoelectron Spectroscopy studies as shown in Fig.1.4.1. The reaction rate as indicated by the surface concentration of oxygen shows an inverse dependence on temperature.

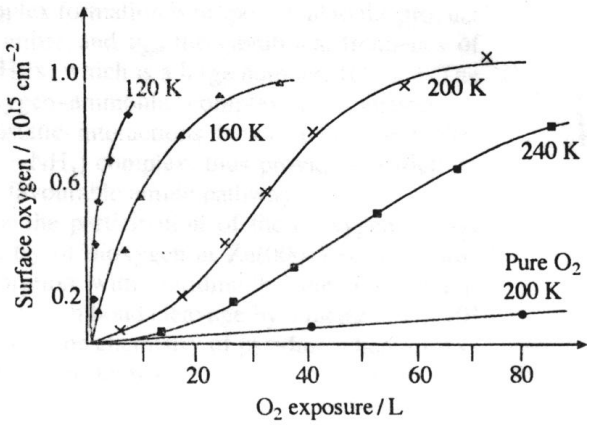

Fig.1.4.1 Variation of surface oxygen (chemisorbed oxygen and hydroxy species) at four temperatures, 240, 200, 160 and 120K as a function of oxygen exposure when a Zn(0001) surface is exposed to ammonia-dioxygen (2:1) mixture (L=Langmuir). Also shown is the data for pure oxygen (From M.W. Roberts, Chemical Society Reviews (1996) 437).

Coadsorption of CO and NH_3 on Ru(0001) surface

Carbon monoxide is known to adsorb on Ru(0001) at both atop and 3-fold sites [44]. When coadsorbed its adsorption on the atop site is inhibited and only the 3-fold site is favoured. With the N-atom in ammonia molecule strongly interacting with the substrate atom, the bending frequency of the N-H bond increases. The CO molecule interacts with the NH_3 molecule electronically through the substrate metal atom. The increase in the bending frequency of N-H bond, lowering of the CO frequency and the strengthening of M-N bond revealed from EELS measurements provide evidence for the formation of NH_3-CO surface complex.

In the case of Ni(110) [45] and Ni(111) [46], CO and NH_3 coadsorption results in the C≡O----H-NH_2 hydrogen bonding. On Cu(110) [47], there is a weak interaction between the CO and NH_3 species upon coadsorption.

Coadsorption of HF and H_2O on Ag(110) surface

Coadsorption of water with hydrogen fluoride on an Ag(110) substrate has been studied in order to examine the relationships between intermolecular hydrogen bonding and preferential adsorption at the surface [48]. Hydrogen fluoride adsorbs on Ag(110) surface in two different states as known from TPD measurements - first layer with a desorption temperature of 117K and the multilayer state that desorbs around 111K. Water shows only single desorption peak around 150K. When coadsorbed, the desorption temperature of both are affected depending on the ratio of water and HF. When H_2O/HF > 3, the water desorption temperature is shifted from 138 to 128K and water desorbs first followed by HF. For H_2O/HF > 1, HF desorbs first followed by water . However for H_2O/HF = 1, the desorption peak of H_2O and HF overlap indicating the formation of a HF.H_2O complex. On Ag(110), the mixed adlayer forms an azeotrope, identified as such by the desorption of both species at temperatures higher than for either species adsorbed alone. By analogy with azeotropes in typical binary solutions, desorption of the two species occurs at constant composition. This is confirmed by the overlap of the desorption curves of water and hydrogen fluoride in the TD spectra for a 1:1 ratio, which shows the strong direct interaction of the two species forming HF.H_2O complex. Here Ag(110) acts as an inert surface where the interaction between the HF and Ag(110) is overwhelmed by the HF-H_2O interactions.

1.5 Experimental methods

Surface Science techniques

There have been many surface specific techniques developed over the last three decades in order to study and understand surface processes and properties. The primary requirement of the surface probe is that it should monitor the properties in the molecular level and should be sensitive to detect over smaller number of atoms. The techniques have been developed successively for higher energy resolution, shorter time scales and atomic level spatial resolution. X-ray Photoelectron Spectroscopy (XPS), Ultraviolet Photoelectron Spectroscopy (UPS), Electron Energy Loss Spectroscopy (EELS), Low Energy Electron Diffration (LEED) and Scanning Tunneling Microscopy (STM) are some of the important surface science techniques. Among the electronic spectroscopic techniques known X-ray Photoelectron Spectroscopy (XPS) is the most popular for the analysis of the surface composition [49]. The work carried out in this thesis is based on XPS.

Photoelectron Spectroscopy

Photoelectron spectroscopy uses a monochromatic photon beam which causes the ejection of a photoelectron out of the sample (time scale ~10^{-16}sec). The kinetic energy of the emitted electron is measured with respect to the Fermi level and the binding energy E_B of the electron from the energy conservation equation is given by

$$h\nu = E_B + E_k + \phi$$

Where E_k is the kinetic energy of the emitted photoelectron and ϕ is the work function of the solid.

If the incident radiation is an X-ray photon beam (AlKα = 1486.6eV or MgKα =1253.6eV) the technique is called as X-ray Photoelectron Spectroscopy (XPS). If the encident energy used is in the ultraviolet region (He I = 21.2eV or He II = 40.8eV) then the technique is known as Ultraviolet Photoelectron Spectroscopy (UPS). XPS is used to probe both the core level and the valence levels whereas UPS finds application in studying the valence band with much higher intensity as well as resolution. XPS is sensitive to ~0.1ML thickness of the substrate. The escape depth of electrons is ~25Å which makes this technique highly surface specific.

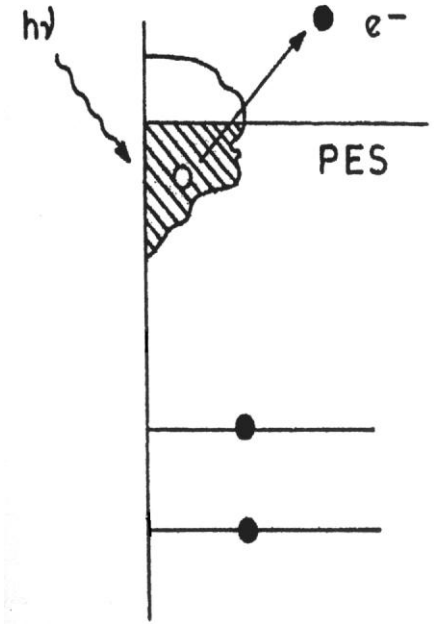

Fig.1.5.1 Schematic diagram showing the emission process

Normally, XPS process will give rise to a single peak corresponding to the removal of an electron, from a single final electronic state. However, the photoemission process is inherently a many-electron event; during photoemission all of the other electrons in the system

must re-adjust their positions and energy since they are no longer in their ground electronic states. Thus, new electronic states become accessible to the final state electrons. These effects give rise to asymmetric peak shapes and various peak widths as well as peak splittings [50]. The different effects are discussed below.

Spin-Orbit Splitting

It occurs due to the coupling of spin and orbital angular momentum of the electron. Spin-orbit separation exists also in initial states and these are well characterized for inner shells. For a closed shell $l > 0$, two sub-shells arise with j quantum numbers $l+1/2$ and $l-1/2$. The relative intensities of the two lines are the statistical weights (2J+1) of the two final states. The splitting increases with Z roughly as a function Z^5. No spin-orbit splitting occurs with s sub-shells.

Multiplet Splitting

Multiplet splitting also referred as exchange splitting of core level peaks can occur when the system has unpaired electrons in the valence. It is found most intensely in 3s (and 4s) peaks when unpaired electrons are present in 3d (and 4f) orbitals. As an example, in the case of Mn^{2+} ion when one of the 3s-electron is ejected, the remaining unpaired electron can interact with the 5 unpaired 3d-electrons in two ways. If the 3s-electron spin is parallel to that of 3d-electrons then exchange interaction can occur, resulting in a lower energy than for the case of anti-parallel spin. Thus, the core level will be a doublet and the separation of the peaks is the exchange interaction energy. Multiplet splitting has considerable potential as a diagnostic probe of the oxidation/spin state, paramagnetic systems and distribution of unpaired electrons.

Jahn-Teller Splitting

If a molecule has complete symmetry, e.g., CH_4, then removal of an electron from one of its degenerate orbitals will remove the electronic symmetry and consequently its degeneracy and the molecular ion may be found in more than one final electronic state. This is known as the Jahn-Teller effect and the energy separation between the final states as Jahn-Teller splitting.

Multielectron Excitations

After creation of a core hole, the reorganization of the electronic structure in the valence shell may also lead to the formation of excited states. If an electron is excited to higher lying bound states, the corresponding satellite lines in the spectrum are called shake-up satellites. If the excitation occurs in to a free continuum states, leaving behind a doubly ionized atom with holes in the core as well as in the valence shell, this effect is known as a shake-off process. Shake-up has been studied mostly for transition metal ions of the 3d series, strong satellites being observed on the 2p lines for the paramagnetic species. Satellites can be used as a reliable guide to oxidation state/spin state in these systems.

Plasmon Excitation

Another final state effect which can influence the shape of the photoelectron spectra, is the occurrence of various inelastic scattering events that the photoelectron experiences as it passes through the solid. The most common of these is the discrete energy loss due to plasmon excitation. Plasmon related feature is observed as a satellite to the main peak in many solids. Free electron metals such as Na and Al exhibit high intensity plasmon features. Besides the above, XP Spectrum may be complicated due to the satellites that could arise from a non-

monochromatic X-ray source and also due to the ghost features from the impurities in the X-ray source.

Instrumentation

While conducting a photoemission experiment, the maintainence of vacuum in the sample environment is highly essential. The photoelectron ejected from the surface of the sample should meet as few molecules as possible on their way to an analyser so that they are not scattered and are lost from the analysis. The mean free path of the electron in the chamber therefore, should be much greater than the dimensions of the spectrometer. In many experiments, it is also necessary to have an atomically clean surface. Since even a very small contamination can affect the course of the experiment drastically, maintainence of vacuum becomes inevitable to reduce the rate of accumulation of contaminants in the time scale of the experiment. Generally, the pressure is kept below ~10^{-10} torr so that the sample surface is accessible for experiments lasting for say, an hour.

All the XPS measurements reported in this thesis have been carried out using a ESCA3 MkII spectrometer of VG Scientific Ltd. (Sussex, UK). Schematic diagram of the spectrometer is shown in Fig.1.5.2. The spectrometer also houses a few other facilities, LEED and STM. It is fitted with a preparatory chamber, the main spectrometer chamber and an anti-chamber. The main chamber and the preparatory chamber are pumped independently using combinations of diffusion and rotary pumps attached with liquid nitrogen traps. The anti-chamber is maintained at a rotary pump vacuum (10^{-3} torr). The sample is transferred to the main chamber via the anti-chamber and preparatory chamber through the gate-valves and is mounted at the end of a stainless steel sample probe. The sample could be resistively heated to 850K through tungsten filaments and also there is provision for cooling it down to 80K using liquid nitrogen.

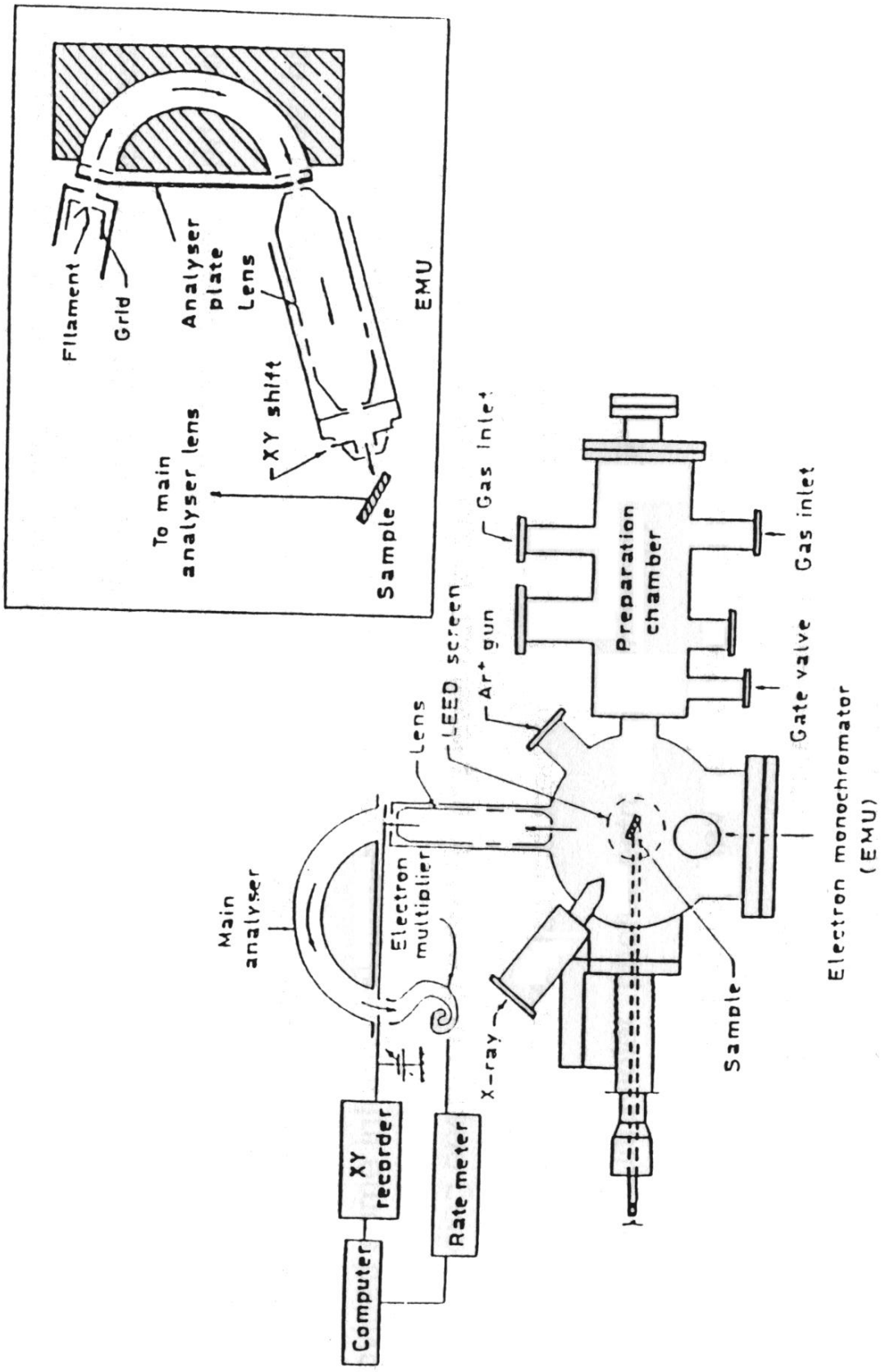

Fig.1.5.2 Schematic diagram of the spectrometer

In order to achieve UHV it is necessary to outgas the walls of the chambers at a faster rate. For this purpose the whole system is heated to 150°C for 24 hours using baking jackets prior to an experiment.

A concentric hemispherical electron analyser (CHA) is used for electron energy analysis (Fig.1.5.3). A deflecting electrostatic field in the analyser disperses the electron energies so that for any given field only those energies in a certain narrow range are measured. Such a field is created using two concentric hemispheres of mean radius R_0 mounted with the common center. A potential V.R is applied between the surfaces so that the outer is negative and the inner is positive with respect to $V.R_0$ which is the median equipotential surface between the hemispheres. The entrance and exit slits are both centered on R_0. If E is the kinetic energy of an electron travelling in an orbit of radius R, then the general expression between E and V is given by

$$EV = E(R_2/R_1 - R_1/R_2)$$

The voltages applied on the inner and outer hemispheres are V1 and V2 respectively and these are given by,

$$V1 = E_0(2R_0/R_1 - 1)$$

$$V2 = E_0(2R_0/R_2 - 1)$$

Where E_0 is the mean analysing energy or pass energy of the analyser. This produces an inverse squared ($1/R^2$) electrostatic field in the region between the hemispheres. The kinetic energy can be scanned either by varying the retardation ratio whilst holding the analyser

energy constant (known as Fixed Analyser transmission or FAT) or by varying the varying the pass energy E_0, whilst holding the retard ratio constant (known as Fixed Retard Ratio or FRR).

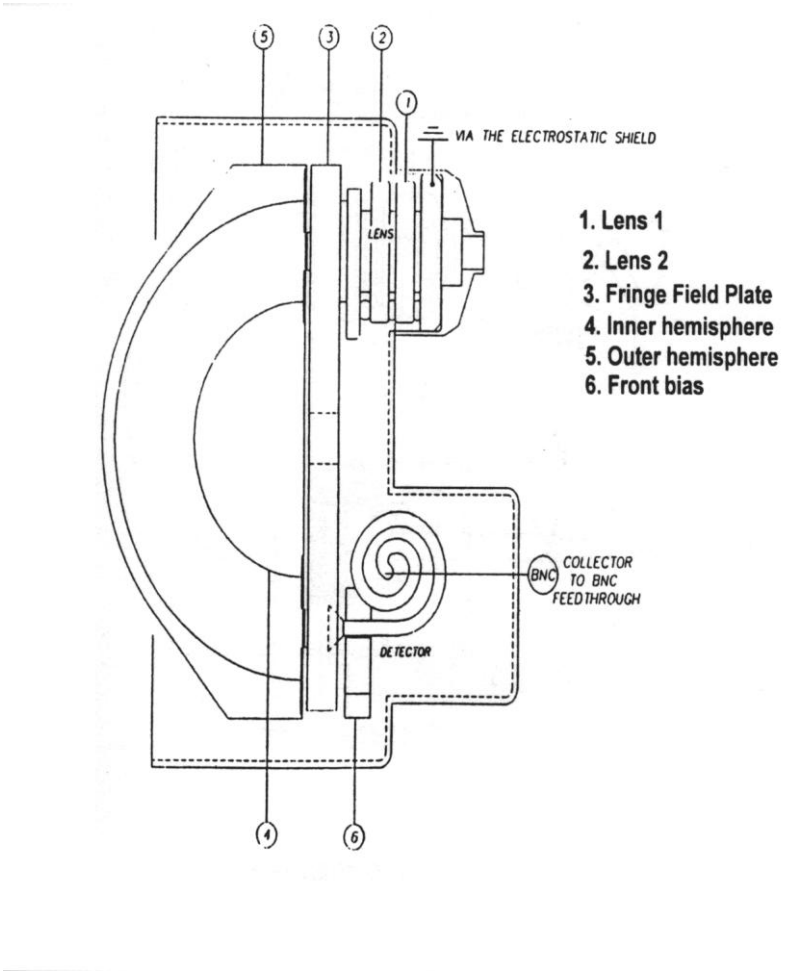

X-ray source

The source of X-ray photon is the X-ray tube that contains a twin anode (Fig.1.5.4) capable of producing both MgKα and AlKα radiations and the radiations pass through a filter made of Al. The X-ray filament is held near the earth potential and the anode at a high positive potential. The X-ray tube is pumped differentially using an ion pump. The anode is cooled by circulating water.

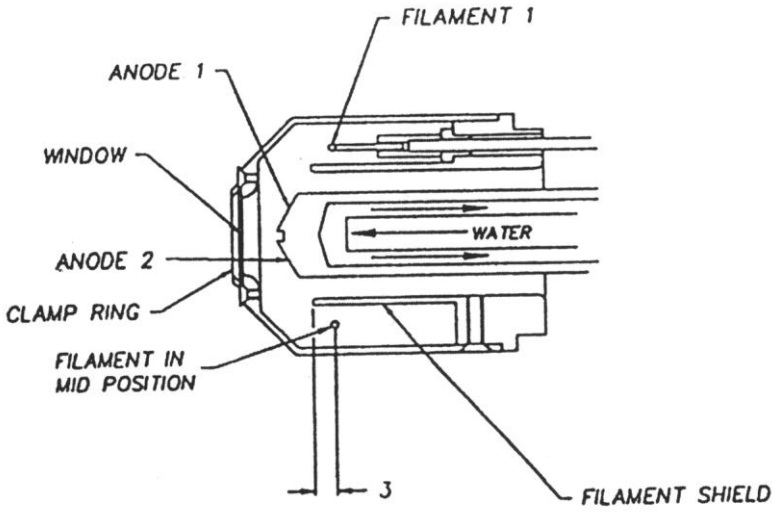

Fig. 1.5.4 Schematic diagram showing the X-ray source

Preparation of the surface

The sample that has been pretreated for cleaning with emmery paper followed by ultrasonification would have carbon, nitrogen, oxygen adsorbed from atmosphere and sometimes sulphur and chlorine as well. These could be removed by an ion etching process. An ion beam of energy is generated in the range 500- 5000eV using an ion gun (Fig. 1.5.5). Usually, Ar gas is used for this purpose. Typically, etching for a period of 30 minutes should produce a clean surface but highly amorphizied. The surface is then heat treated to two thirds of its melting point for few minutes in order to facilitate reconstruction. This process is called annealing. However, many times the contaminants from the bulk may diffuse to the surface during annealing. This difficulty can be overcome by repeating the sputtering and annealing cycles a few times.

Once a well-formed surface is ready, the required molecules are dosed using sensitive fine leak valves at a pressure below 10^{-5} torr.

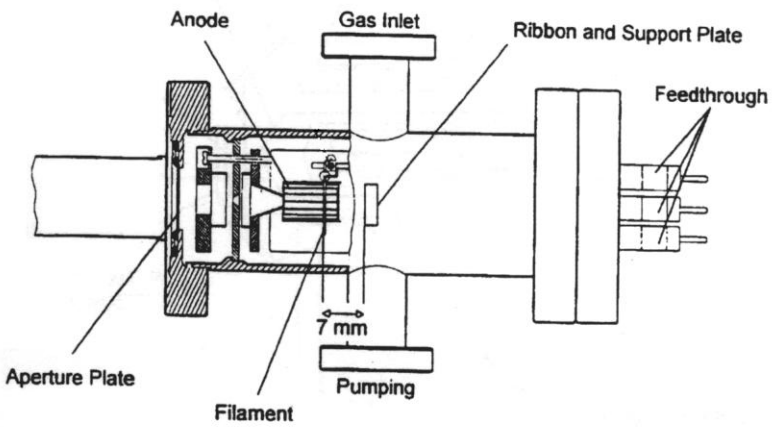

Fig1.5.5 Schematic diagram showing the essential parts of a typical Argon ion gun

Quantitative XPS:

It is well known that the XP spectral technique is used for the quantitative analysis of the adsorbate on the surface other than qualitative composition analysis. It is used to measure the surface area of the substrate, surface coverage and thickness of the adsorbed layer and the concentration of various adsorbed species. If one wants to calculate the coverage of gas molecules or atoms on the surface (σ), a formula due to Carley and Roberts is used [51]. This is valid upto a coverage less than a monolayer only.

$$\sigma = \frac{I_{ads}\ K.E_{ads}\ N_A\ \rho_{sub}\ \mu_{sub}\ \lambda_{ads}\ \cos\phi}{I_{sub}\ \mu_{ads}\ M_{sub}\ K.E_{sub}}$$

Here I's correspond to the photoelectron intensity of the adsorbate and substrate, K.E's correspond to the kinetic energy of the photoelectron of the adsorbate and the substrate. N_A is the Avagadro number, ρ is the density of the substrate, M is the molecular mass of the substrate, μ is the photoelectron cross section [52]. λ is the mean free path of the substrate electrons in the matrix of the adsorbate and ϕ is the angle of collection of photoelectrons with respect to surface normal. For multilayer coverages, spectral intensity normalized with respect to the cross section serves as a simple measure of the population of a given species.

1.6 Scope of the present investigations

Surface chemistry of molecules continues to be an area of great interest with immediate relevance to heterogeneous catalysis and electrochemistry. The nature of the species produced on metal surfaces and their reactivity patterns are the main ongoing activities in our laboratory. The present work addresses two such issues.

1. A hydrogen bonded methanol-water complex

The adsorption of methanol is dissociative even on relatively inert surfaces such as Zn(0001). Earlier work in this laboratory has shown that methanol adsorbed on a clean Zn(0001) surface at 80K, dissociates into methoxy species on warming to 120K and eventually to hydrocarbon species above 150K. Our aim in this work was to examine if molecular methanol could be stabilized in an hydrogen bonded network involving water molecules. The Zn(0001) surface is well suited for our study in that the surface chemistry of methanol is purely temperature dependent and that water shows negligible reactivity with the Zn(0001) surface. We considered that coadsorption experiments using mixtures of methanol and water in varying proportions would be ideal for this purpose. This study gains more relevance in the light of the cluster beam studies on methanol-water system carried out in this laboratory recently [53]. The present belongs to a class of very few that deal with surface mediated hydrogen bond.

2. Coadsorption of CS_2 and O_2

CS_2 is a linear molecule, which can have as many as three adsorption sites, two from sulphur and one from carbon on a metal surface. CS_2 adsorption at room temperature is therefore, dissociative especially on reactive surfaces such as Ni(100). We have chosen to study CS_2 adsorption on Ni(110) surface, which is hitherto unknown. Besides pure CS_2,

coadsorption of CS_2 and O_2 on Ni(110) is expected to bring out interesting surface reactivity pattern. Indeed, dioxygen adsorption on Ni(110) produces a significant proportion of O^{1-} species which can grab transient species from a second molecule to form new species on the surface [54]. An investigation of the interaction between CS_2 and O_2 on Ni(110) is therefore, worthwhile.

1.7 References

[1] Hammer, B and Norskov, J K Nature 376 (1995) 238.

[2] G.A. Somarjai, Introduction to Surface Science and Catalysis, Wiley Interscience, 1994

[3] J.W. May, Adv.Catal. 21 (1970) 151.

[4] D.P. Woodruff, T.A. Delchar, Modern Techniques of Surface Science, Cambridge Solid State Science Series, Cambridge University Press, New York 1986.

[5] P.W. Atkins, Physical Chemistry Oxford University Press Oxford Melbourne Tokyo, 1998.

[6] J.V. Barth, Surf. Sci. Rep. 40 (2000) 75.

[7] B.J. Behm, G. Ertl and V. Panka, Surf. Sci. 160 (1985) 387.

[8] R.J. Koestner, M.A. Van Hove and G.A. Somarjai, Surf. Sci. 107 (1981) 439.

[9] D.F. Ogletree, M.A. Van Hove and Somarjai, Surf. Sci. 173 (1986) 351.

[10]C.N.R. Rao, K.Prabhakaran and M.K. Rajumon, Reviews of Solid State Science, 4, No.4 (1990) 843.

[11]C.T. Au, A.F. Carley, A. Pashuski, S. Read and M.W. Roberts, In adsorption on ordered surfaces of Ionic Solids and Thin Films; Springer Series in Surface Science, 33 Springer - Verlag: Berlin and Heidelberg, Germany (1994) 241.

[12]G.U. Kulkarni, C.N.R. Rao and M.W. Roberts, J.Phys.Chem. 99 (1995) 3310.

[13]G.U. Kulkarni, C.N.R. rao and M.W. Roberts, Langmuir 11 (1995) 2572.

[14]K. Wandelt, Surf. Sci. Rep. 2 (1982) 1.

[15]D. Schmeisser and K. Jacobi, Surf. Sci. 156 (1985) 911.

[16]C.T. Au, S.S. Boparai, and M.W. Roberts, J. Chem. Soc. Farad. Trans. I 79 (1983) 1779.

[17]C.T. Campbell and M.T. Pafett, Surf. Sci. 146 (1984) 256.

[18]P. R. Norton, Surf. Sci. 47 (1975) 98.

[19]J.L. Gland, B.A. Sexton and G.B. Fisher, Surf. Sci. 95 (1980) 587.

[20]C.N.R. Rao and G. Ranga Rao, Surf. Sci. Rep. 13 (1991) 221.

[21]F. Bozzo, G. Ertl, M. Grunze and M. Weiss, J. Catal. 49 (1977) 18.

[22]W. Diekmann, G. Panzner and H.J. Grabke, Surf. Sci. 218 (1989) 507.

[23]N.D. Spencer and G.A. Somorjai, J. Catal. 78 (1982) 142.

[24]N.D. Spencer and G.A. Somorjai, J. Phys. Chem. 86 (1982) 3493.

[25]G. Haase and M. Asscher, Surf. Sci. 191 (1987) 75.

[26]T. Kioka, H. Miki and K. Kawasaki, Surf. Sci. 130 (1983) L294.

[27]G.J. Dooley III and T.W. Haas, Surf. Sci. 19 (1970) 1.

[28]M.J. Grunze, J. Fuhler, M. Neumann, C.R. Brundle, D.J. Auerbach and J. Behm, Surf. Sci. 139 (1984) 109.

[29]M. Wilf and P.T. Dawson, Surf. Sci. 60 (1976) 561.

[30]D.A. King and F.C. Tompkins, Trans. Faraday Soc. 64 (1968) 496.

[31]E. Fromm and O. Mayer, Surf. Sci. 74 (1978) 259.

[32]Y. Kuwahara, M. Jo, H. Tsuda, M. Onchi and M. Nishijima, Surf. Sci. 180 (1987) 421.

[33]Patricia A. Thiel, Surf. Sci. Rep. 7 (1987) 211.

[34]T.E. Madey and J.T. Yates, Jr., Chem. Phys. Letters 51 (1977) 77.

[35]H. Ibach and S. Lehwald, Surf. Sci. 91 (1980) 187.

[36]Andersson, C. Nyberg and C.G. Tengstal, Chem. Phys. Lett. 104 (1984) 305.

[37]K. Jacobi, K. Bedurftig, Y. Wang, G. Ertl, Surf. Sci. 472 (2001) 9.

[38]C. Nobel, C. Benndorf and T.E. Madey, Surf. Sci. 157 (1985) 29.

[39]C. Benndorf and T.E. Madey, Surf. Sci. 194 (1988) 63.

[40]M. Polak, Surf. Sci 321 (1994) 249.

[41]Padalia B.D., Gimzewski J.K., Affrossman S., Lang W.C., Watson L.M. and Fabian D.J., Surf. Sci. 61 (1976) 468.

[42]Fuggle J.C., Watson L.M., Fabian D.J. and Affrossman S., Surf. Sci. 49 (1975) 61.

[43]M.W. Roberts, Chemical Society Reviews (1996) 437.

[44]Y. Zhou, S. Akhter and J.M. White, Surf. Sci. 202 (1988) 357.

[45]M.J. Dresser, A.M. Lanzillotto, M.D. Alvey and J.T. Yates, Jr., Surf. Sci 191 (1987) 1.

[46]A.M. Lanzillotto, M.J. Dresser, M.D. Alvey and J.T. Yates, Jr., Surf. Sci.191 (1987) 15.

[47]D. Lackey and D.A. King, J. Chem. Soc. Faraday Trans. 83 (1987) 2001.

[48]A. Krasnopoler, N. Kizhakevariam and E. M. Stuve, J. Chem. Soc., Faraday Trans., 92, No.13 (1996) 2445.

[49]D. Briggs and M.P. Seah, Practical Surface Analysis Volume 1, Second edition, John Wiley & Sons, UK.

[50]R.I. Hegde and P.B. Sinha, Appl. Spec. Rev. 19 (1983) 1.

[51]A.F. Carley and M.W. Roberts, Proc. R. Soc. London A 363 (1978) 403.

[52]J.H. Scofield, J.Electron Spectros. 8 (1976) 129.

[53]G. Raina, G.U. Kulkarni, Chem. Phys. Lett. 337 (2001) 269.

[54]G.U. Kulkarni, C.N.R. Rao, M.W. Roberts, J. Phys. Chem. 99 (1995) 3310.

Chapter 2

A hydrogen bonded methanol-water complex on Zn(0001) surface

2.1 Introduction

Hydrogen bonds in molecular solids and liquids have been investigated extensively in the last few decades. Although a knowledge of hydrogen bonding at metal-solvent interfaces is of great importance in electrochemical and corrosion processes, such studies are rather rare [1]. One of the important aspects that is related to surface hydrogen bonds is, how a metal surface mediates a hydrogen bond that could increase the stability of a species or a complex, that is otherwise unstable under a given set of conditions. Such situations usually arise while adsorbing two different species on the surface. For example, Krasnopoler et al.[2] studied coadsorption of water with either NH_3 or HF on a Ag(110) substrate and found that water not only enhanced the population of the chemisorbed state of ammonia, but also increased the average desorption temperature by as much as 21K from 134K. In contrast, hydrogen fluoride and water form a well defined monohydrate $HF.H_2O$, as evidenced by the coincident thermal desorption curves of both species.

We considered it to be interesting to investigate how water may stabilize methanol molecules via hydrogen bonds on a Zn(0001) surface. It is known from the earlier studies by Rao and co-workers [3] that methanol dosed on a Zn(0001) surface at 80K, adsorbs molecularly forming both the chemisorbed and the physisorbed species. On warming the surface to 120K, the physisorbed molecules desorbed and the chemisorbed species transformed to methoxy species.

$$CH_3OH \longrightarrow CH_3O(a) + H(a)$$

On further heating to 150K, the C-O bond scission takes place forming hydrocarbon species which is stable upto room temperature.

$$CH_3O(a) \longrightarrow CH_3(a) + \tfrac{1}{2} O_2$$

The Zn(0001) surface is well suited for our study in that the surface chemistry of methanol is purely temperature dependent. Moreover, water shows negligible reactivity with Zn(0001) surface [4]. It adsorbs moleculary on Zn(0001) surface at low temperatures and desorbs neatly at 200K. Our intention was to study the influence of the O-H---O hydrogen bonds between water and methanol on the chemisorbed states of the latter. For this purpose, we have exposed the Zn(0001) surface at 80K, to the binary vapors from water-methanol liquid compositions of 90:10, 70:30 and 50:50, and obtained the C1s, O1s and Zn(2p) core level spectra at 80K as well as at elevated substrate temperatures. Our work has indeed shown that water stabilizes molecular methanol upto 200K via hydrogen bond interaction.

2.2 Experimental

Photoelectron spectroscopy measurements were carried out using a VG ESCA3 MkII spectrometer fitted with a sample preparation chamber at a base pressure of ~$2x10^{-10}$ torr. AlKα (1486.6eV) was employed as the incident radiation. Adsorption studies were carried out on the (0001) face of a single crystal of Zinc (purity of 99.99%) obtained from Atomergic Chemicals Corporation (UK). The surface was cleaned by Ar^+ ion etching (beam energy, 2.5keV) followed by annealing at ~ 450K until a clean surface, devoid of carbon and oxygen, was obtained.

Methanol used in the study was of spectroscopic grade (HPLC grade, Aldrich) and was further purified for dissolved gas impurities on a UHV gas handling system through several freeze-pump-thaw cycles. Double distilled water used in the experiment was also subjected to freeze-pump-thaw cycles. Water-methanol liquid mixtures with water mole fractions, x_w, of 0.5, 0.7 and 0.9 were prepared in test tubes. The vapor from the mixtures was dosed into the preparation chamber using fine-leak valves. Around 30L (1L = 10^{-6} torr.sec) of exposure was found sufficient to obtain a monolayer coverage of the species. The C1s, O1s and Zn2p core-level spectra were collected at 80K and also at several temperatures during warming the surface to room temperature. The experimental data were fitted with multiple gaussian peaks to extract out the intensities of corresponding species.

2.3 Results and discussion

In Fig.2.3.1 we show the C1s and O1s spectra of 12L of methanol adsorbed on the Zn(0001) surface at 80K, which was subsequently warmed to room temperature. At 80K, we observe intense peaks in C1s and O1s centered around 288.0 and 534.3eV respectively characteristic of physisorbed methanol molecules [5,6]. The slight asymmetry seen in the spectra at lower binding energy arises due to a small proportion of the chemisorbed species $CH_3OH(a)$. On warming the surface to 120K, the peaks decrease in intensity and develop new features on the lower energy side. Deconvoluted spectra show the presence of the chemisorbed methanol (C1s, 287; O1s, 533.5eV) and the methoxy species (C1s, 286; O1s, 532eV) along with condensed methanol. Thus, a rise in the surface temperature causes proton abstraction. The methanol molecules desorb almost entirely around 150K. Now, the methyl or more correctly, the CH_x species ($x \leq 3$) at ~285eV is seen on the surface arising from the C-O bond scission of the methoxy species, the proportion of which increases as the temperature is risen.

In a separate experiment, a 20L of water was dosed on a clean Zn(0001) surface at 80K (see Inset of Fig.2.3.1).

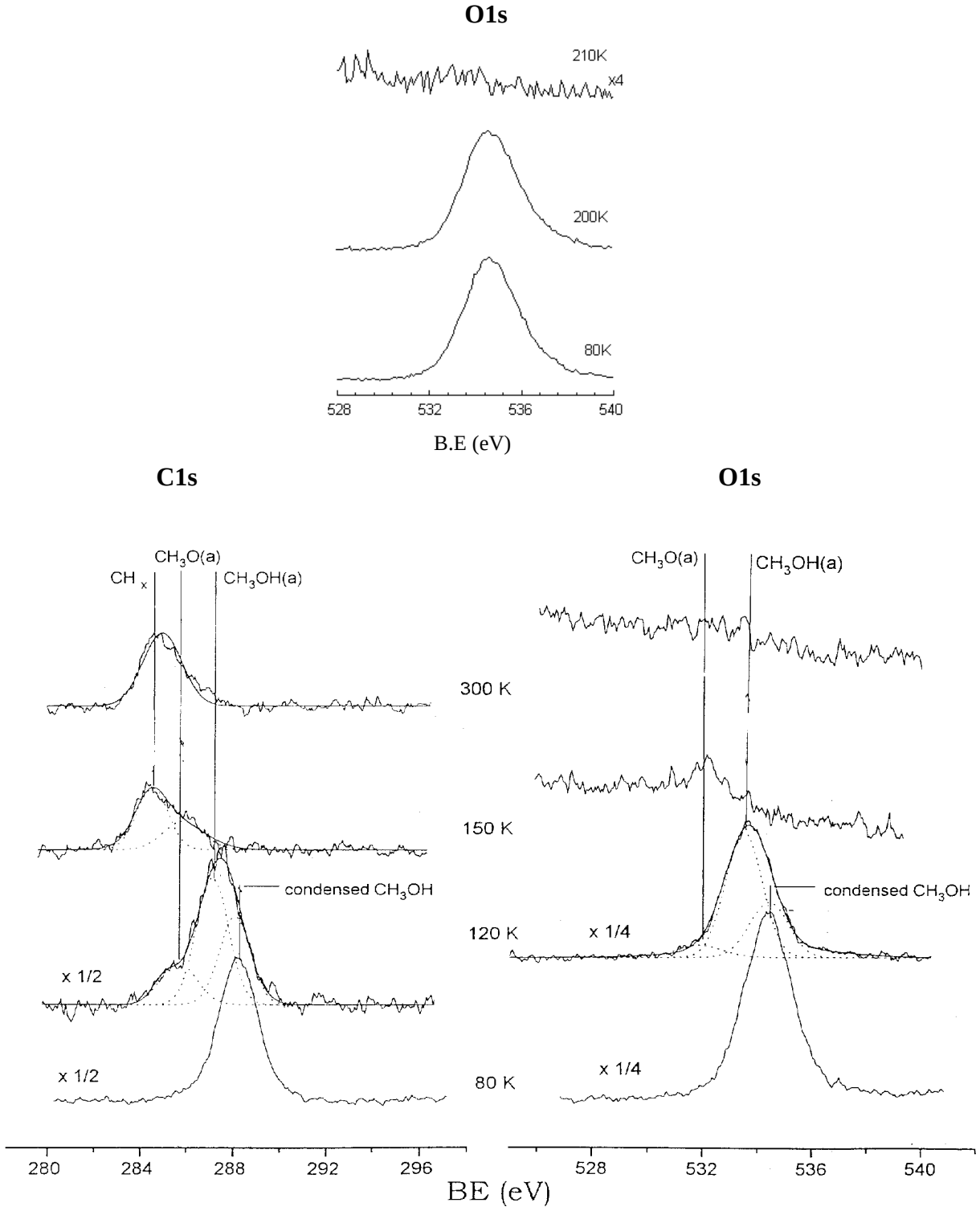

Figure 2.3.1 C1s and O1s spectra of methanol adsorbed on a Zn(0001) surface. Methanol (12L) was first adsorbed at 80K and the surface was gradually warmed to 300K. Inset shows the O1s spectra of water adsorbed on Zn(0001) surface at 80K and after warming to 210K.

We see a single peak in the O1s region at 533.5eV due to the physisorbed water, which remains unchanged while warming to 200K. Above this temperature, no peak was observed in the O1s region, indicating that water molecules desorbed neatly from the surface without any dissociation.

The Zn(0001) surface exposed to vapor mixtures of methanol and water were examined in a similar way. Figures 2.3.2 to 2.3.4 refer to the experiments conducted using methanol-water liquid mixtures with water molefraction, x_w, of 0.5, 0.7 and 0.9 respectively. For x_w=0.5 at 80K, the C1s and O1s spectra in Fig.2.3.2 show broad but intense peaks centered around 287.6 and 533.6eV respectively, characteristic of molecular methanol and water on the surface. The C1s peak is slightly broader compared to pure methanol adsorption (Fig.2.3.1). On warming the surface gradually to 100K, the peaks become less intense and broaden. The C1s peak becomes visibly asymmetric on the lower energy side due to the emergence of the methoxy species at 286eV. At 150K, the C1s peak shifts to ~285eV with a wide shoulder at the higher binding energy side. On further heating the surface to room temperature, the shoulder almost vanishes leaving behind a peak centered around 285eV due to the CH_x species. Accordingly, the intensity of the O1s spectrum becomes negligible. It is clear from the figure that the molecular methanol species leave the Zn surface gradually when the temperature is above 100K, some of them dissociating to the methoxy and the CH_x species, the latter being relatively more at higher temperatures similar to pure methanol adsorption (Fig.2.3.1). What is interesting is that with x_w=0.5, the molecular methanol species is seen upto 180K in clear contrast to pure methanol adsorption. Thus, it appears that both the proton abstraction from methanol and the C-O bond scission processes are delayed when water is co-adsorbed with methanol. Beyond 200K, the methanol species desorb leaving behind methoxy and CH_x species.

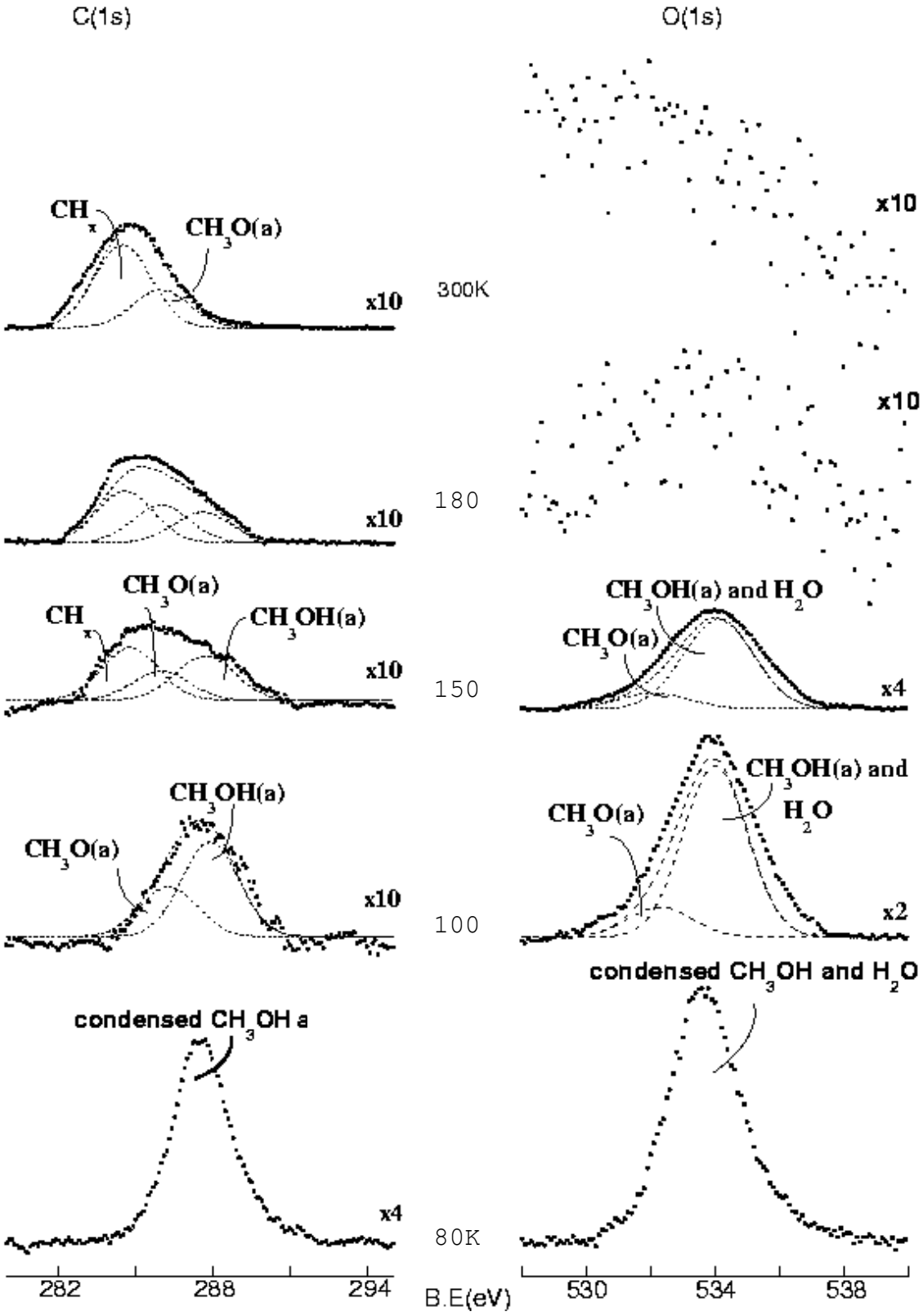

Figure 2.3.2 C1s and O1s spectra obtained after exposing Zn(0001) surface at 80K to a water-methanol vapor (30L) from a liquid mixture with x_w=0.5. Effect of warming to higher temperatures is also shown.

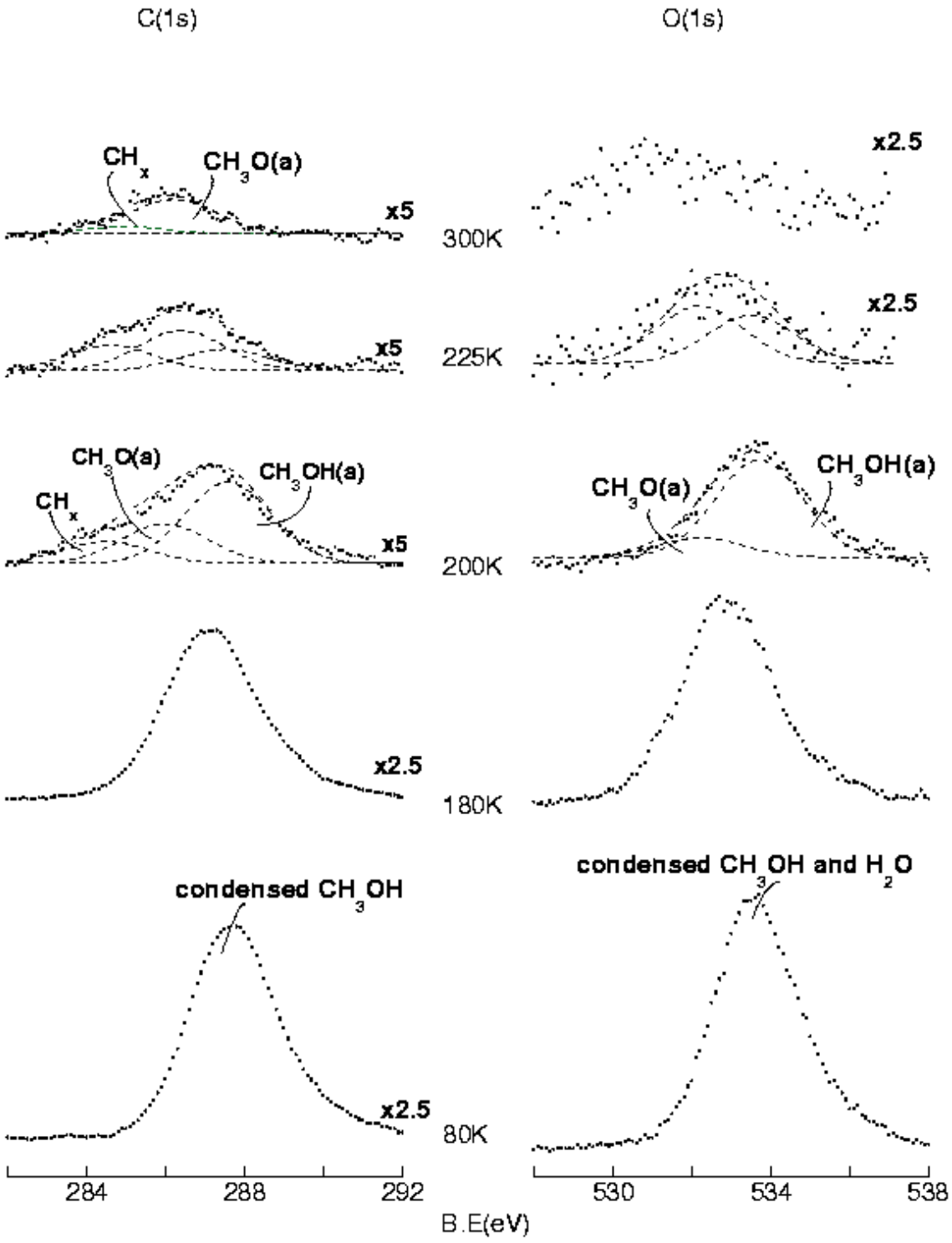

Figure 2.3.3 C1s and O1s spectra obtained after exposing Zn(0001) surface at 80K to a water-methanol vapor (20L) from a liquid mixture with x_w=0.7. Effect of warming to higher temperatures is also shown.

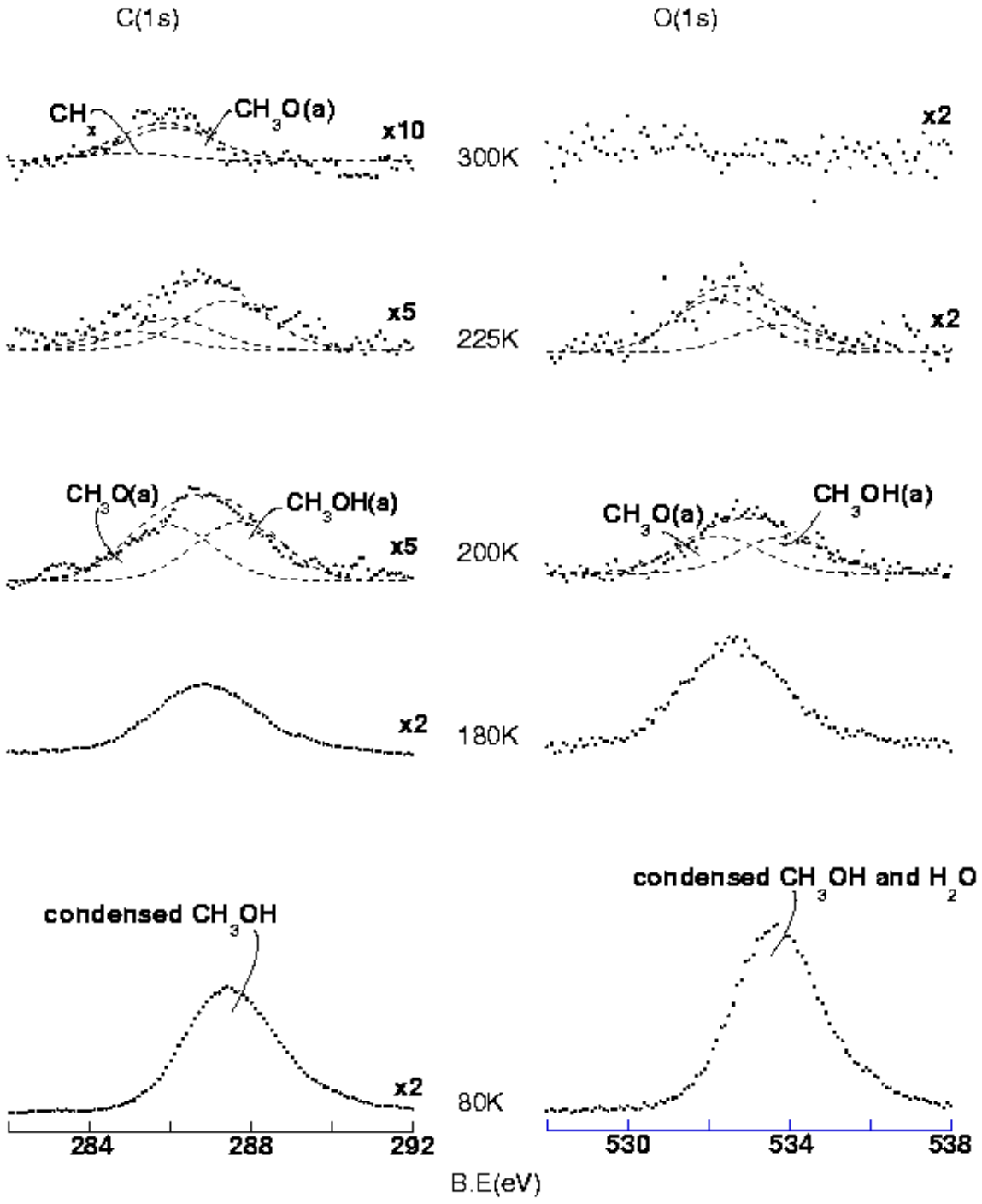

Figure 2.3.4 C1s and O1s spectra obtained after exposing Zn(0001) surface at 80K to a water-methanol vapor (20L) from a liquid mixture with x_w=0.9. Effect of warming to higher temperatures is also shown.

Figure 2.3.3 shows the XP spectra obtained when a clean Zn(0001) surface was exposed at 80K to 30L of the vapor from the water–methanol mixture with x_w of 0.7, and subsequently warmed to room temperature. At 80K, the C1s and O1s spectra appear similar to those obtained with x_w of 0.5 (Fig.2.3.2). Interestingly, even after warming the surface to 150K, we observed essentially no changes in the spectral intensities and shapes. At 180K however, both the peaks shift towards lower binding energies by ~0.7eV accompanied by some broadening. The overall intensities decrease only slightly. At 200K, the C1s peak begins to exhibit asymmetry due to the emergence of methoxy and CH_x species at 286 and 285eV respectively. At this temperature, the methanol peak at 287.5eV is comparable in intensity to that in the case of x_w=0.5 at 100K. The O1s peak also decreased in intensity and became broader due to the emergence of methoxy species at 532.5eV. Above 200K, we still see a peak due to methanol but of lower intensity, the peak due to methoxy species being relatively higher. At 300K however, no molecular methanol was seen, the predominant peak being due to the methoxy species. The O1s region shows same intensity due to the methoxy species at 532.5eV.

The spectra obtained with x_w=0.9 are shown in Fig.2.3.4. At 80K, the C1s (287.5eV) and O1s (533.7eV) peaks appear less intense than obtained with x_w=0.7 but are comparable to those with x_w=0.5. On warming, the peaks remain unchanged upto 180K except for some decrease in intensity above 135K. However, on reaching 180K, the peaks broaden and shift by ~0.6eV towards lower binding energies and the intensities reduce considerably. At 200K, the methoxy and the methanol species are equal in intensity. Unlike in the case of x_w =0.7 (Fig.2.3.3), no CH_x species was seen at this temperature. Warming to 225K results in further decrease in the intensities of methanol and methoxy species.

In Fig.2.3.5, we show how the intensities of C1s and O1s spectra normalized with respect to the values at 80K, vary with temperature in the above experiments. For x_w=0 (pure methanol adsorption), both C1s and O1s intensities drop sharply reaching a small value (~0.1) around 150K. The drop in the intensities are rather sharp for x_w=0.5 as well. On the other hand, for higher values of x_w (0.7 and 0.9), we see a different trend. The curves corresponding to x_w=0.9 fall off gradually with rise in temperature beyond 150K. Interestingly, in the case of x_w=0.7, the C1s and O1s curves remain virtually close to 1.0 till ~200K and follow a trend much like a first order phase transition. Beyond 200K, the variations in the C1s intensities are gradual. It may be noted that the variations in O1s intensity in the case of x_w=0.7 and 0.9 are comparable to that of pure water (x_w=1.0) itself (see Fig.2.3.5b). Thus, it appears that water molecules stabilize methanol molecules on the Zn(0001) surface, the extent of which depends critically on the the relative proportions of the two.

In the insets of Fig.2.3.5, we have shown variations of the C1s and O1s intensities corresponding to the molecular methanol species. It is indeed striking that the methanol variation resembles closely variations in the total intensities, especially below 200K, implying that methanol molecules stabilized by water are the preponderant species on the surface. However, following water desorption above 200K, the dissociation of methanol molecules sets in. The methoxy species are found to be relatively more abundant in mixtures with x_w of 0.7 and 0.9 while the CH_x species dominate with the x_w = 0.5 mixture.

An accurate estimation of surface concentrations of water and methanol at low temperatures from the condensed multilayers was not possible due to limited probing depth of XPS. The relative surface concentrations of water and methanol species at 80 K was calculated by taking the ratio of the intensities normalized with respect to the cross sections.

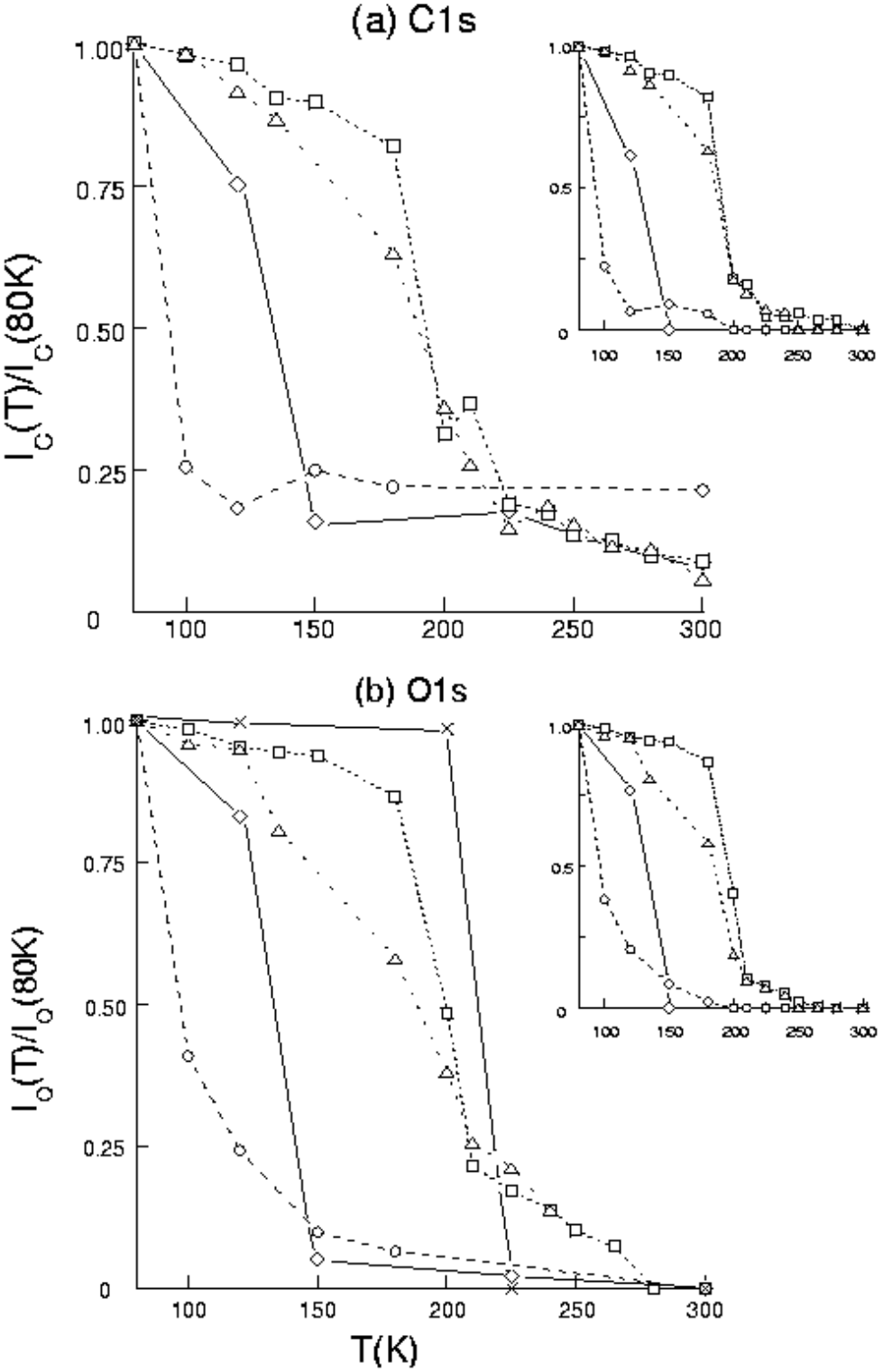

Figure 2.3.5 Variation in (a) the relative C1s intensity (b) the relative O1s intensity with temperature, x_w = 0 (diamonds), 0.5 (circles), 0.7 (squares), 0.9 (triangles) and 1.0 (crosses). The insets show the corresponding variations arising from molecular methanol species

Thus, the ratio of the concentrations of methanol and water on the surface was estimated to be close to one for both x_w = 0.7 and 0.9 compositions, while for x_w of 0.5, a value of 0.6 was obtained.

We have seen from Fig.2.3.5 that the adlayer obtained with x_w of 0.7 is highly stable and a sharp transition occurs at around 200K when the whole layer desorbs at once while that with x_w of 0.9 breaks and allows molecules to desorb and dissociate, although the latter contains a similar ratio of water and methanol molecules (1:1). This observation implies that the internal structure of the two adlayers is different. It is likely that the adlayer obtained with x_w of 0.7 comprises of an intimately bonded water and methanol molecules in the form of a hydrogen bonded network. The methanol molecules are retained on the Zn surface by the water molecules up to 200 K, beyond which the latter themselves desorb. The scenario is different for x_w of 0.9 in that there appears to be some clustering of water molecules on the surface and therefore, their promotional effect in stabilizing methanol is not much. The above observations go very well with our recent cluster beam studies on the structure of water-methanol liquid mixtures [7]. These studies have shown that the mixture with x_w of 0.7 consists of extended hydrogen bond network in the liquid between water and methanol where each methanol is surrounded water molecules and vice versa. The condensed layer in this experiment behaves in the expected way. It may be recalled that this mixture is also the one where the excess enthalpy of mixing is minimum among other compositions due to increased water-methanol hydrogen bonding.

2.4 Conclusions

1. When the Zn(0001) surface is exposed to pure methanol at 80K, only molecular species is present. On warming to 120K, the physisorbed species desorb leaving behind the chemisorbed species. Besides methoxy species are found on the surface, which upon further heating give rise to CH_x species due to the C-O bond cleavage.
2. When a binary vapor is dosed, water and methanol molecules coexist on the Zn surface due to the surface mediated hydrogen bonding. The stabilization of molecular methanol in the form of a water-methanol complex is so strong that the dissociation and desorption of methanol is inhibited upto 200K, beyond which water itself desorbs. Such a stabilization of methanol molecule is very efficient in the case of water-rich mixtures, especially for x_w = 0.7.
3. Both hydrogen abstraction from chemisorbed methanol and C-O bond scission take place much more gradually when water molecules are present alongside methanol on the surface. Methoxy and CH_x appear only around 200K for x_w=0.7 and 0.9, while they appear slightly earlier at ~150K in the case of x_w = 0.5.
4. Above 200K, CH_x species is dominant in the case of x_w=0.5, its concentration is the least for x_w=0.9, the latter surface being more abundant with the methoxy species.

2.5 References

[1] Patricia A. Thiel, Surf. Sci. Rep. 7 (1987) 211.

[2] A. Krasnopoler, N. Kizhakevariam and E. M. Stuve, J. Chem. Soc., Faraday Trans. 92 (1996) 2445.

[3] K.R. Harikumar, C.P. Vinod, G.U. Kulkarni, and C.N.R. Rao, J. Phys. Chem. B 103 (1999) 2445.

[4] I. Abbati, L. Braicovich, B. De Michelis and A.Fasana, Solid State Commun. 26 (1978) 515.

[5] T.S. Rufael, J.D. Batteas and C.M. Friend, Surf. Sci. 384 (1997) 156.

[6] M.K. Wedon, P. Uvdal, C.M. Friend and J.G. Serafin, J.Chem. Phys. 103 (1995) 5075.

[7] G. Raina, G.U. Kulkarni, Chem. Phys. Lett. 337 (2001) 269.

Chapter 3

Interaction between carbon disulphide and oxygen on a Ni(110) surface

3.1 Introduction

Studies that deal with the interaction of CS_2 with metal surfaces are only a few in the literature. Yagi et al. [1-3] investigated using S K -edge X-ray absorption fine structure spectrscopy and X-ray photoelectron spectroscopic techniques, the adsorption of CS_2 on Cu(100) and Cu(111) at low temperatures and found that the adsorption is molecular. However, the same authors working with Ni(100) [4] surface concluded that CS_2 readily dissociates and forms atomic carbon and sulphur at low coverages. However, there was no evidence of any intermediate adsorbed species such as CS(a). It was of our interest to study the dissociation pathway of CS_2 on a Ni(110) surface. This being on more open surface compared to Ni(100), the interaction of CS_2 is expected to be stronger.

We have carried out coadsorption experiments using dioxygen as a probe molecule in order to trap and interact intermediary dissociation species of CS_2. It may be recalled that oxygen on Ni(110) produces O^{1-} species besides O^{2-} (oxidic) species, the former being reactive [5]. For this purpose, we exposed clean Ni(110) surface to CS_2-O_2 mixtures with compositions of 220:1, 15:1 and 2:1 at room temperature and recorded X-ray photoelectron spectra in the O1s, C1s, S2p and Ni2p core level regions. We have also performed experiments where CS_2 and O_2 were adsorbed sequentially. Our study has shown that the O^{1-} transient species interact with CS_2 to give rise to carbonyl sulphide species on the surface.

3.2 Experimental

Photoelectron spectroscopy measurements were carried out using a VG ESCA3 MkII spectrometer fitted with a sample preparation chamber at a base pressure of ~$2x10^{-10}$ torr. AlKα (1486.6eV) was employed as the incident radiation. Adsorption studies were carried out on a (110) surface of a single crystal nickel (purity of 99.99%) polished using a polishing machine (Phoenix Beta, Wirtz Buehler, Germany). The surface was cleaned by repeated cycles of Ar^+ ion etching (beam energy 3.5keV) and annealing at ~450^oC until a clean surface, devoid of carbon oxygen and sulphur was obtained.

Spectroscopic grade CS_2 and ultrahigh pure grade O_2 were used after purification by means of freeze-pump-thaw cycles. CS_2:O_2 mixtures were prepared using a gas handling system and the compositions were measured using a quadrupole mass spectrometer (SRS RGA 300, CA, USA). The compositions of the three CS_2-O_2 mixtures prepared were 220:1, 15:1 and 2:1 respectively.

3.3 Results and discussion

In Fig.3.3.1 we show the C1s, S2p and Ni2p spectra recorded after exposing the Ni(110) surface to 20L of pure CS_2 at room temperature. The C1s region exhibits an intense peak at 285eV which is slightly asymmetric on the higher binding energy side. The S2p peak appears at ~164eV and is quiet broad because the spin-orbit splitting between $p_{3/2}$ and $p_{1/2}$ levels is within the instrumental resolution. The reported C1s and S2p binding energies for molecular CS_2 are ~287 and ~163.6eV respectively [6]. The C1s binding energy in the present case is however, much lower. This perhaps corresponds to a situation where CS_2 is mostly dissociated into graphitic carbon (285eV), a chemisorbed sulphur species (164eV) as in the case of Ni(100) surface [4].

$$CS_2 \xrightarrow{Ni(110)} C(a) + 2S^{2-}(a) + 2Ni^{2+}$$

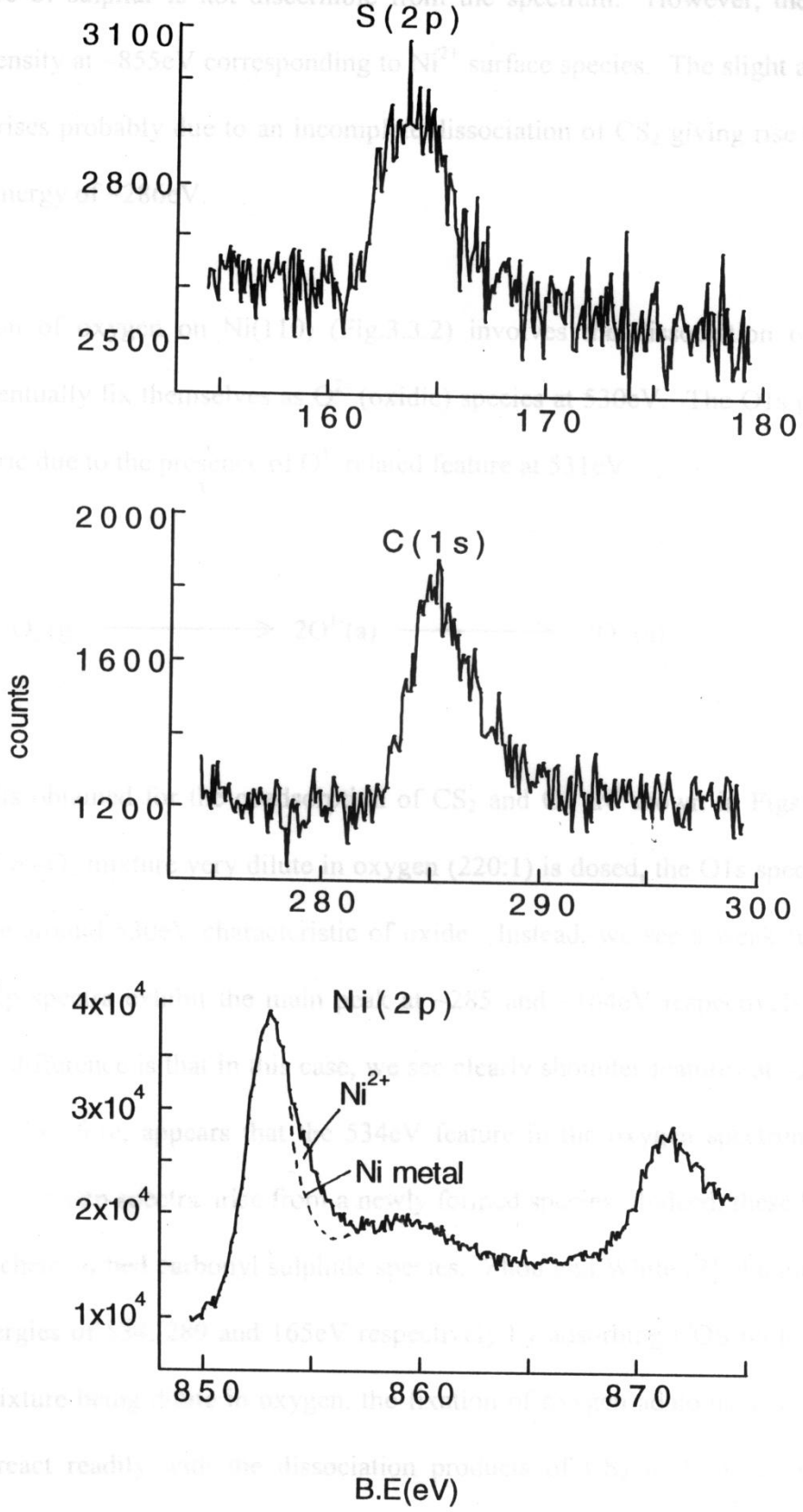

Figure 3.3.1 XP spectra in the S2p, C1s and Ni2p regions after dosing 20L of pure CS_2 on a Ni(110) surface at room temperature.

The exact nature of sulphur is not discernible from the spectrum. However, the Ni2p spectrum shows some intensity at ~855eV corresponding to Ni^{2+} surface species. The slight asymmetry in the C1s spectrum arises probably due to an incomplete dissociation of CS_2 giving rise to CS(a) species with a binding energy of ~286eV.

Adsorption of oxygen on Ni(110) (Fig.3.3.2) involves the dissociation of dioxygen into adatoms that eventually fix themselves as O^{2-} (oxidic) species at 530eV. The O1s peak is however, highly asymmetric due to the presence of O^{1-} related feature at 531eV.

$$O_2\,(g) \longrightarrow 2O^{1-}(a) \longrightarrow 2O^{2-}(a)$$

The results obtained for the coadsorption of CS_2 and O_2 are shown in Figs.3.3.3, 3.3.4 and 3.3.5. When a CS_2-O_2 mixture very dilute in oxygen (220:1) is dosed, the O1s spectrum (Fig.3.3.3) shows no feature around 530eV characteristic of oxide. Instead, we see a weak feature at 534eV. The C1s and S2p spectra exhibit the main peak at ~285 and ~164eV respectively as in pure CS_2 adsorption. The difference is that in this case, we see clearly shoulder features at ~287 and ~166eV respectively. It, therefore, appears that the 534eV feature in the oxygen spectrum as well as the shoulders in C1s and S2p spectra arise from a newly formed species. Indeed, these binding energies correspond to a chemisorbed carbonyl sulphide species. Zhou and White [7] obtained O1s, C1s and S2p binding energies of 534, 289 and 165eV respectively by adsorbing COS molecule on Ag(111) surface. The mixture being dilute in oxygen, the fixation of oxygen adatoms as oxide is inhibited. The transients react readily with the dissociation products of CS_2 to form a carbonyl sulphide species,

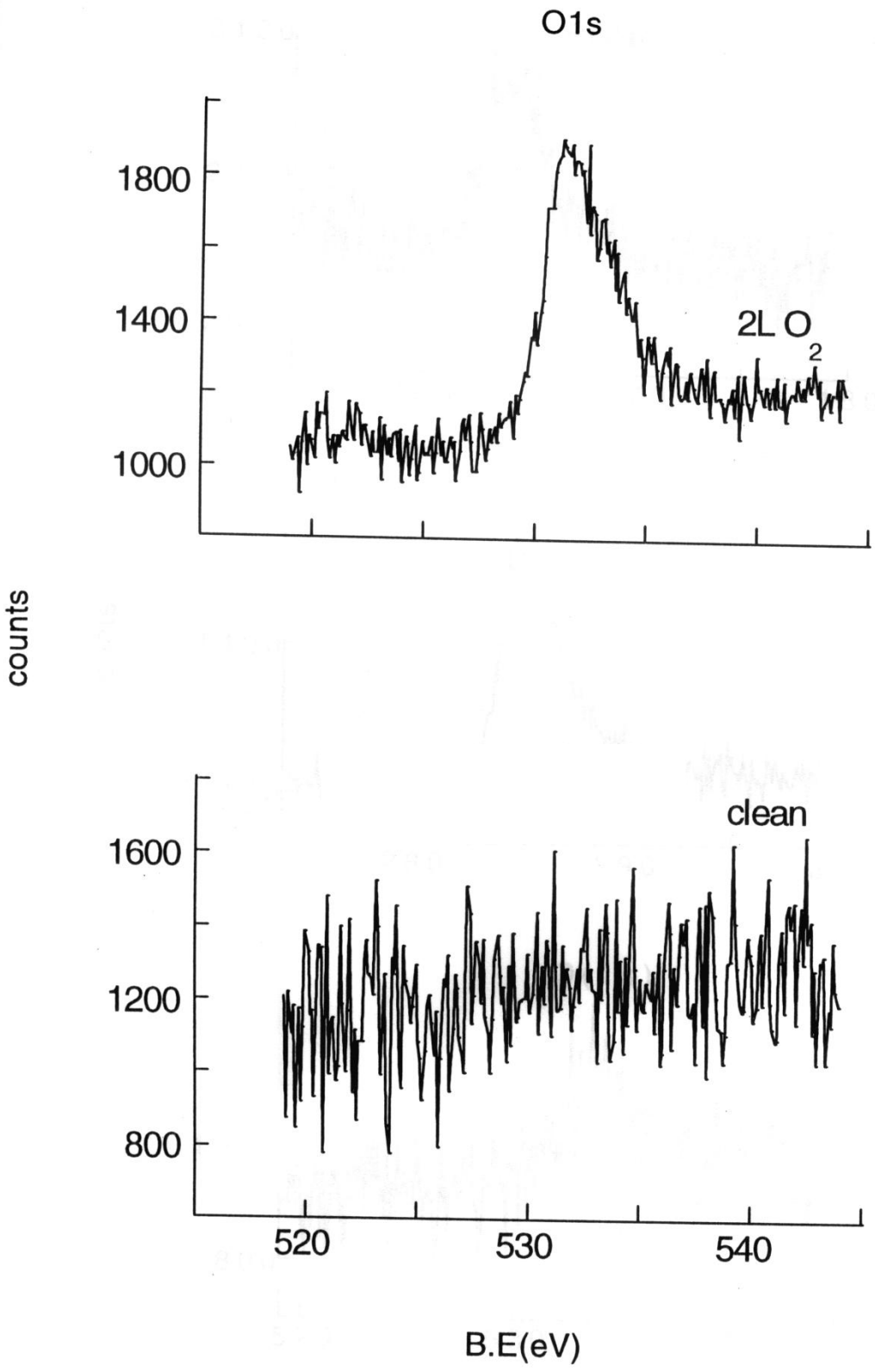

Figure 3.3.2 XP spectra in the O1s region after dosing 2L of O_2 on Ni(110) surface at room temperature.

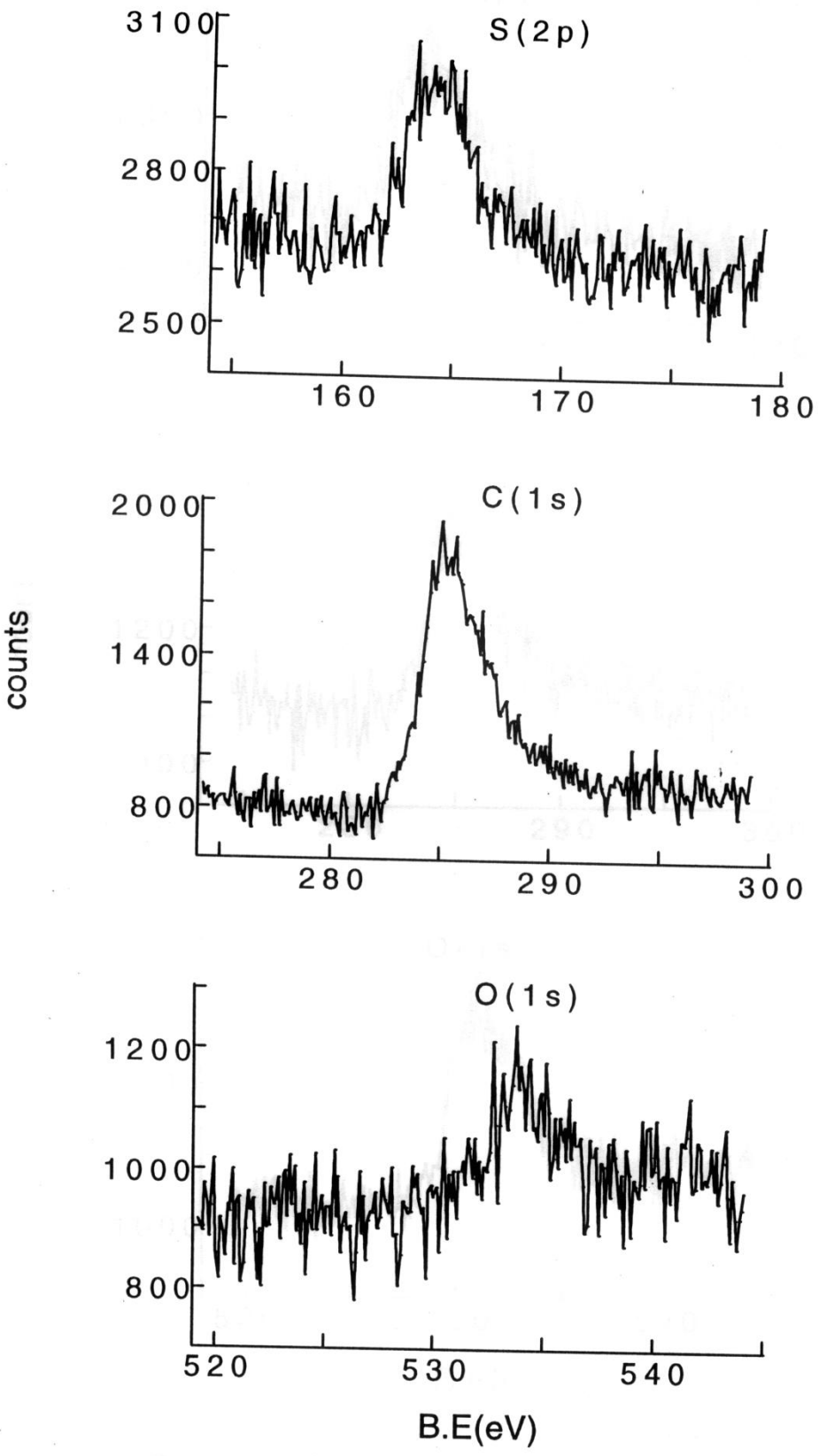

Figure 3.3.3 XP spectra in the O1s, C1s and S2p regions after dosing 20L of the 220:1 mixture of CS_2:O_2 on a Ni(110) surface at room temperature.

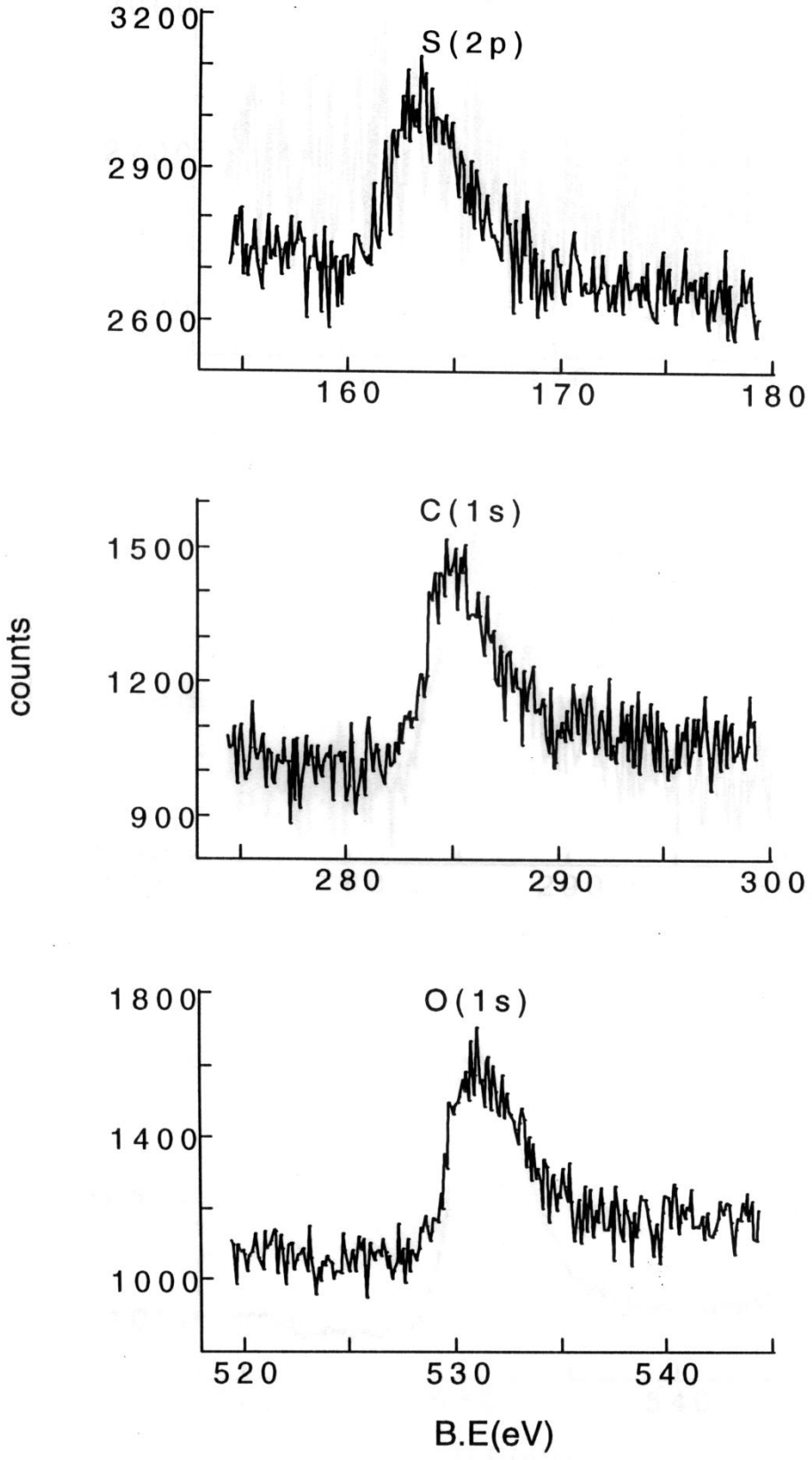

Figure 3.3.4 XP spectra in the O1s, C1s and S2p regions after dosing 20L of the 15:1 mixture of CS_2:O_2 on a Ni(110) surface at room temperature.

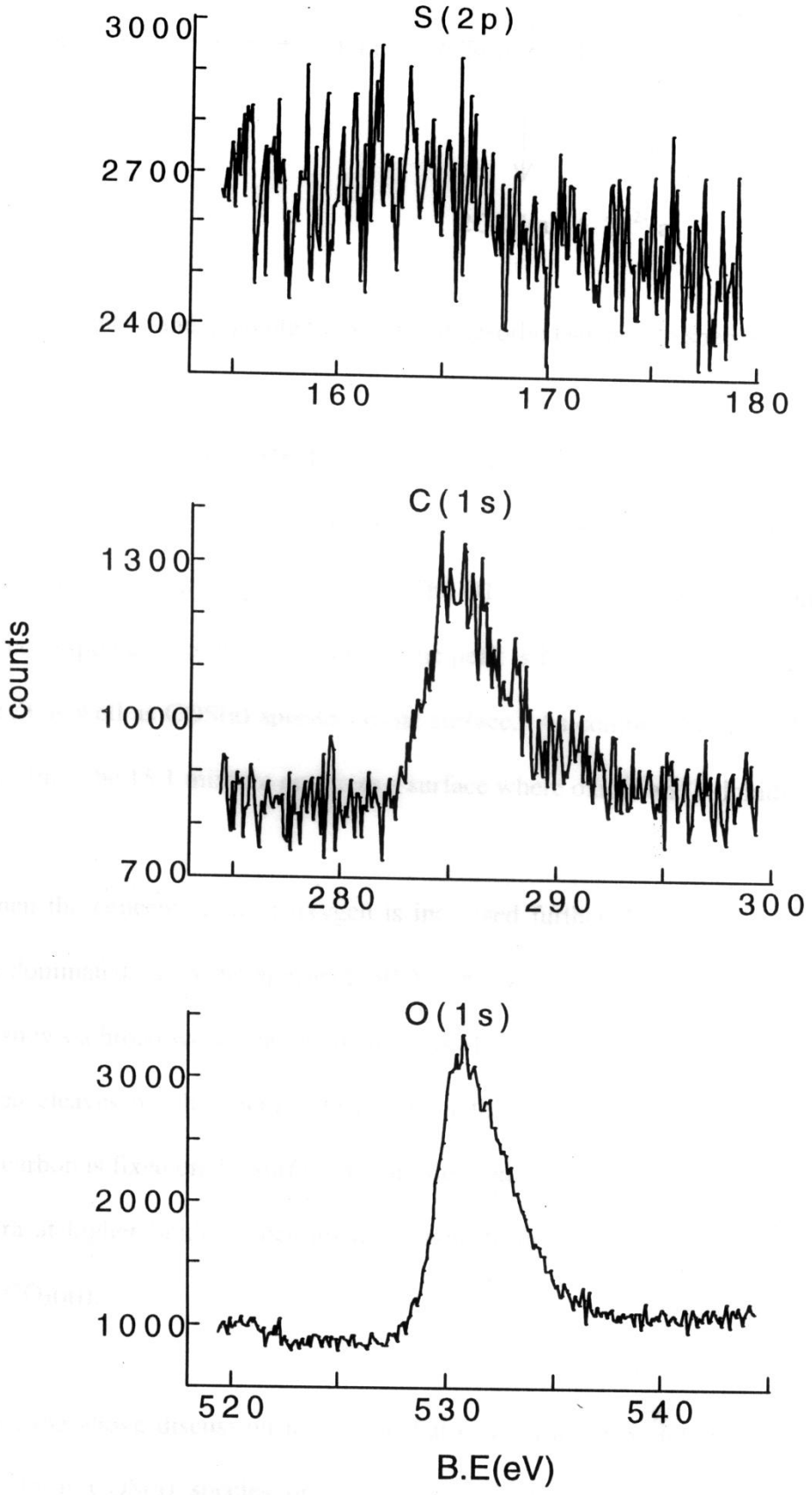

Figure 3.3.5 XP spectra in the S2p, C1s and O1s regions after dosing 20L of the 2:1 mixture of CS_2:O_2 on a Ni(110) surface at room temperature.

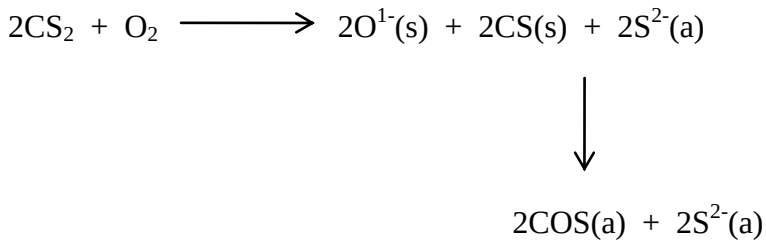

where the subscripts s and a denote transient and adsorbed species, respectively.

Figure 3.3.4 shows the O1s, C1s and S2p spectra after exposing a clean Ni(110) surface to a 15:1 mixture of CS_2-O_2. The C1s and S2p spectra are similar to those in Fig.3.3.3 although the intensity of C1s feature is somewhat lower. The O1s spectrum in Fig.3.3.4 exhibits a peak centered at 531eV corresponding to the O^{1-} species. The peak is broad (~4eV) indicating that there are some O^{2-} (530eV) as well as COS(a) species on the surface. As compared to the adsorption of the 220:1 CS_2-O_2 mixture, the 15:1 mixture produces a surface where oxidic and sulphidic species coexist.

When the concentration of oxygen is increased further as in the CS_2:O_2 = 2:1 mixture, the surface is dominated by oxidic species (530eV) as seen in the O1s spectrum in Fig.3.3.5 The C1s spectrum shows a broad weak peak while there is virtually no intensity in the S2p region. It appears that oxygen cleaves off the chemisorbed sulphur that had formed during the dissociation of CS_2. Although carbon is fixed on the surface as carbide or graphitic species, the asymmetry in the C1s and O1s spectra at higher binding energies does indicate the formation of oxygenated carbon species (CO(a) or CO_2(a)).

From the above discussion it is clear that oxygen and CS_2 interact during the coadsorption process to form COS(a) species on the surface which are stable, provided oxygen adsorption pathway leading to oxidic species is inhibited as in the case of mixtures very dilute in oxygen. If the proportion of oxygen is comparable to that of CS_2, the oxygen adsorption leads only to the oxidic

(O^{2-}) species. In such a situation not only COS(a) is unstable but also chemisorbed sulphur from CS_2 dissociation is cleaved off from the surface perhaps as SO_2.

In order to establish the role of O^{1-} species in producing COS(a) on the surface, we carried out a sequential adsorption experiment. In the first case, a clean Ni(110) surface was exposed to 2L of oxygen to produce a surface predominant in O^{1-} (a) species (531eV) following which, 20L of CS_2 was dosed (Fig.3.3.6). It is clear from the figures that CS_2 adsorption results in the broadening of the O1s peak at the higher binding energy side along with noticeable intensities in the C1s and S2p regions. In contrast to coadsorption experiments the O^{1-} species (531eV) that are already present on the surface react with CS_2 to give rise to some COS(a) species. However, there are carbon and chemisorbed sulphur species resulting from the dissociation of CS_2. The spectra in Fig.3.3.7 correspond to a situation where CS_2 is adsorbed first followed by oxygen. As we can see clearly, there is not much of reactivity when the surface is exposed to 2L of O_2. But when the exposure is increased to 20L a small intensity at 534eV seen in the spectrum. Since the surface is populated with dissociated products of CS_2, oxygen adsorption is inhibited.

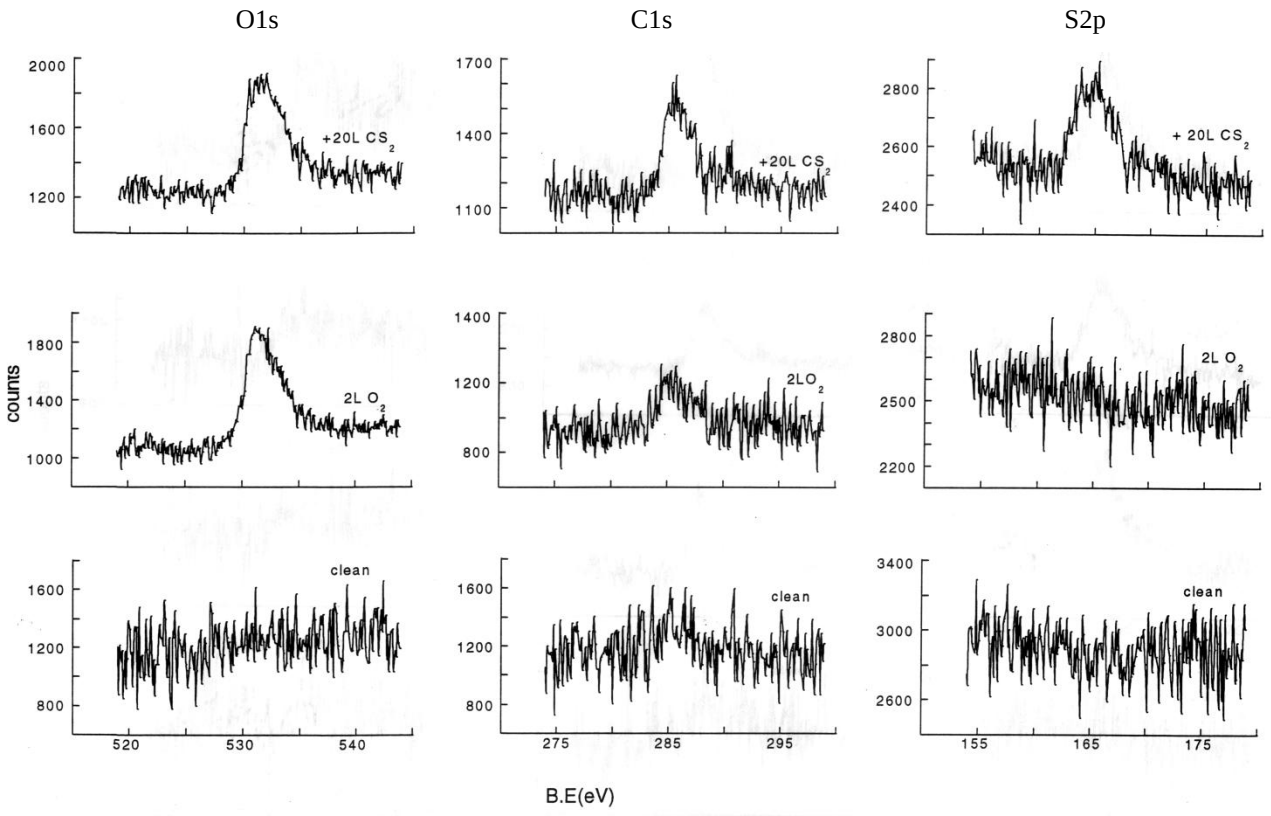

Figure 3.3.6 XP spectra in the O1s, C1s and S2p regions after dosing 2L of O_2 followed by 20L of CS_2 on a Ni(110) surface at room temperature.

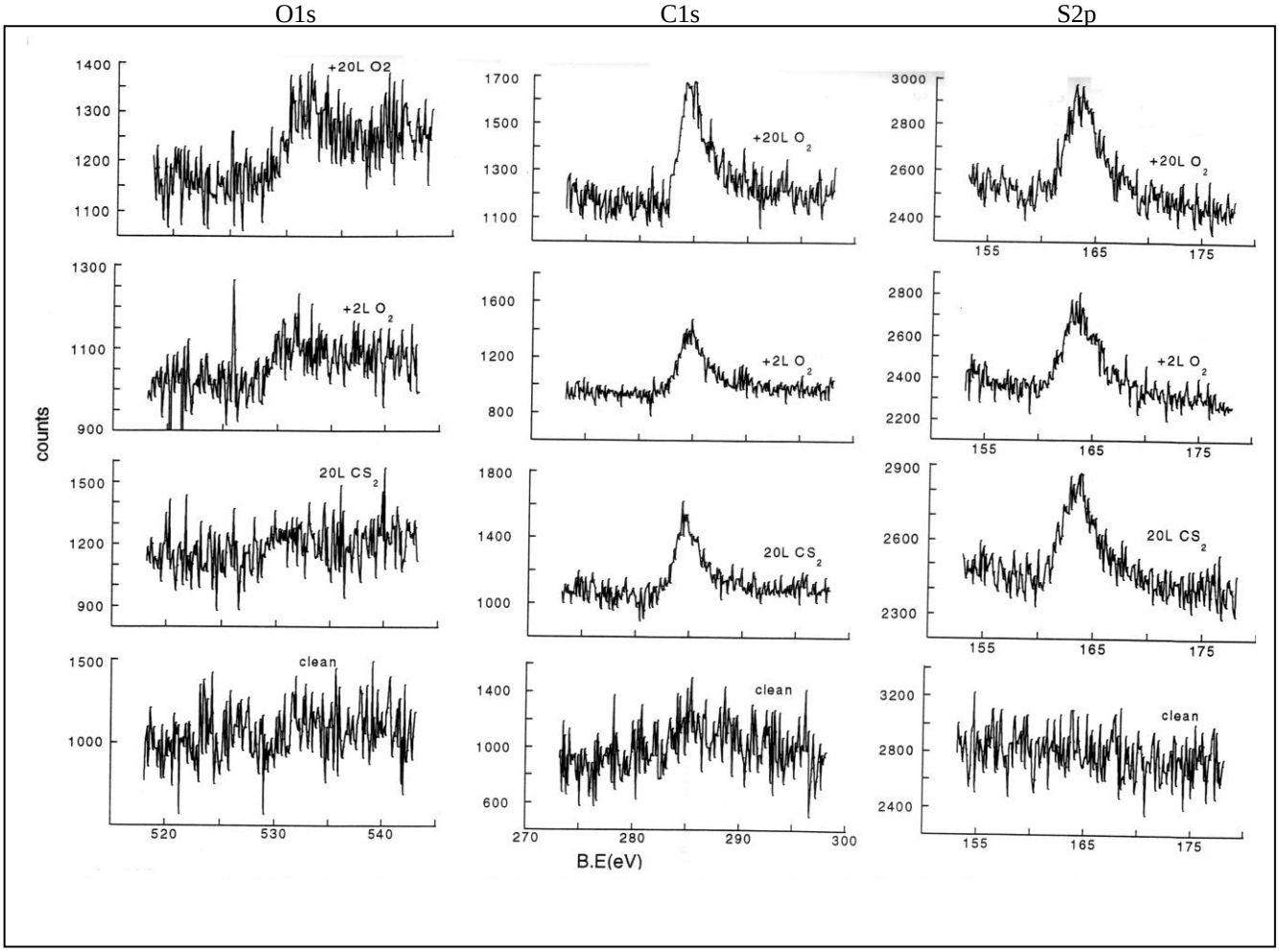

Figure 3.3.7 XP spectra in the C1s, S2p and O1s regions after dosing successively 20L of CS_2, 2L of O_2 and 20L of O_2 on a Ni(110) surface at room temperature.

3.4 Conclusions

1. Pure CS_2 on Ni(110) surface dissociates into graphitic carbon and sulphidic species at room temperature. A small proportion of CS(a) species are also produced.
2. On adsorbing a CS_2-O_2 mixture very dilute in oxygen (220:1), the transient O^{1-}(s) species interacts with CS(s) species to give rise to a new molecule, COS(a).
3. As the oxygen content is increased in the mixture from 220:1 to 15:1, the surface is covered with O^{1-}(a) species in addition to COS(a).
4. Further increase in the oxygen content 2:1 favours the oxidic O^{2-}(a) species. There is no evidence of the COS(a) and S^{2-}(a) species on the surface.
5. The formation of COS is seen also when CS_2 is dosed on a Ni(110) surface containing O^{1-}(a) species produced by exposing the clean surface to 2L of oxygen. On the contrary, a Ni(110) surface predosed with CS_2 does not show much reactivity towards O_2.

3.5 References

[1] S. Yagi, T. Yokoyama, Y.Kitajima, Y. Takata, T. Kanazawa, A. Imanishi, T. Ohta, Surf. Sci. 311 (1994).

[2] S. Yagi, S.Takenaka, T. Yokoyama, Y. Kitajima, A. Imanishi, T. Ohta, Surf. Sci. 325 (1995) 68.

[3] S. Yagi, T. Yokoyama, Y. Kitajima, A. Imanishi, S. Takenaka, T. Ohta, Physica B 208 & 209 (1995) 447.

[4] T. Yokoyama, S. Yagi, Y. Takata, H. Sato, T. Asahi, T. Ohta, Surf. Sci. 274 (1992) 222.

[5] G.U. Kulkarni, C.N.R. Rao, M.W. Roberts, J. Phys. Chem. 99 (1995) 3310.

[6] C.D. Wagner, J.A. Taylor, J. Electron spectrosc. Relat. Phenom. 28 (1982) 211.

[7] X.L. Zhou and J.M. White, Surf. Sci. 235 (1990) 259.